



January 2015

Understanding And Predicting Bagging Performance Through The Use Of CFD And DEM Simulations

Matthew Perry Leone

Follow this and additional works at: <https://commons.und.edu/theses>

Recommended Citation

Leone, Matthew Perry, "Understanding And Predicting Bagging Performance Through The Use Of CFD And DEM Simulations" (2015). *Theses and Dissertations*. 1801.
<https://commons.und.edu/theses/1801>

This Thesis is brought to you for free and open access by the Theses, Dissertations, and Senior Projects at UND Scholarly Commons. It has been accepted for inclusion in Theses and Dissertations by an authorized administrator of UND Scholarly Commons. For more information, please contact zeinebyousif@library.und.edu.

UNDERSTANDING AND PREDICTING BAGGING PERFORMANCE THROUGH
THE USE OF CFD AND DEM SIMULATIONS

by

Matthew Perry Leone
Bachelor of Science, University of North Dakota, 2010

A Thesis

Submitted to the Graduate Faculty

of the

University of North Dakota

in partial fulfillment of the requirements

for the degree of

Master of Science

Grand Forks, North Dakota

May
2015

Copyright 2015 Matthew P. Leone

This thesis, submitted by Matthew Perry Leone in partial fulfillment of the requirements for the Degree of Master of Science from the University of North Dakota, has been read by the Faculty Advisory Committee under whom the work has been done and is hereby approved.



Marcellin Zahui

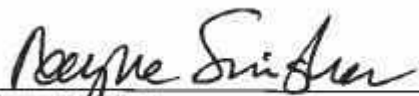


George Bibel

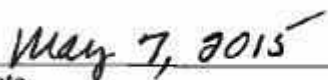


Cai Xia Yang

This thesis is being submitted by the appointed advisory committee as having met all of the requirements of the School of Graduate Studies at the University of North Dakota is hereby approved.



Wayne Swisher
Dean of the School of Graduate Studies



Date

PERMISSION

Title Understanding and Predicting Bagging Performance Through the use of
 CFD and DEM Simulations

Department Mechanical Engineering

Degree Master of Science

In presenting this thesis in partial fulfillment of the requirements for a graduate degree from the University of North Dakota, I agree that the library of this University shall make it freely available for inspection. I further agree that permission for extensive copying for scholarly purposes may be granted by the professor who supervised my thesis work or, in his absence, by the Chairperson of the department or the dean of the School of Graduate Studies. It is understood that any copying or publication or other use of this thesis or part thereof for financial gain shall not be allowed without my written permission. It is also understood that due recognition shall be given to me and to the University of North Dakota in any scholarly use which may be made of any material in my thesis.

Matthew Perry Leone
May 7, 2015

TABLE OF CONTENTS

LIST OF FIGURES	viii
LIST OF TABLES.....	xi
ACKNOWLEDGEMENTS.....	xii
ABSTRACT.....	xiii
CHAPTER	
I. INTRODUCTION	1
Description of Project	1
Need for Project	3
Similar External Projects	3
II. VARIABLE IDENTIFICATION	5
Introduction.....	5
Nature Variables	6
Natural Variables	7
Design Variables.....	8
Mower Deck Variables	9
Material Collection System Variables	11
External Variables.....	12
Summary.....	13
III. TEST MODELS.....	14
Introduction.....	14

Baseline 1	14
Baseline 2	16
Iteration 1	17
Iteration 2	19
IV. AIRFLOW TESTING OVERVIEW	21
Theory Development	21
Test Setup.....	22
Field	22
Virtual	24
Test Method	26
Field	26
Virtual	27
Results – Field & Virtual	27
Baseline 1	27
Baseline 2	29
Iteration 1	30
Iteration 2	32
Summary.....	33
V. PARTICLE TESTING OVERVIEW	35
Theory Development	35
Test Setup.....	36
Field	36
Virtual	36

Test Method	38
Field	38
Virtual	39
Results – Field & Virtual	40
Baseline 1	41
Baseline 2	42
Iteration 1	44
Iteration 2	45
Summary	47
VI. DISCUSSION	48
Grass Types, Grass Heights & Cut Heights	48
MCS Chute Exit Particle Velocities	50
Room for Improvement & Future Opportunities	51
VII. CONCLUSION	53
APPENDICES	54
REFERENCES	64

LIST OF FIGURES

Figure	Page
1. CAD model of the John Deere Select Series X350R Model Year 16 Tractor.....	2
2. Early morning testing weather conditions at the cut plots.....	7
3. CAD model of the X350R Material Collection System.	8
4. Deck shell and deck chute geometries.	9
5. Attack angle and deck rake.	9
6. Mower blade designs.	10
7. Underside view of mower deck.	11
8. Material Collection System Design Variables.....	12
9. CAD model of the B1 design.....	15
10. Cross-section view of the B1 model.	15
11. CAD model of the B2 design.....	16
12. Cross-section view of the B2 model.	17
13. CAD model of the Iter1 design.	18
14. Cross-section view of the Iter1 model.	18
15. CAD model of the Iter2 design.	19
16. Cross-section view of the Iter2 model.	20
17. Mower deck leveling gage.	22
18. Flow measurement locations.....	23
19. Dwyer Instruments, Series 475 Mark 3 Digital Manometer.....	24

20. Flow versus pressure drop of the hopper bag materials.....	25
21. Air data measurement locations taken in the field.....	26
22. CFD flow field locations within the MCS chute.	27
23. Wake regions generated in the Baseline 1 CFD model.	28
24. Velocity reduction regions generated in the Baseline 2 CFD model.....	29
25. Velocity reduction region generated in the Iteration 1 CFD model.....	31
26. Velocity reduction region generated in the Iteration 2 CFD model.....	32
27. Airflow velocity magnitude midway through the hopper.	34
28. Airflow velocity magnitude at the rear of the hopper.....	34
29. Grass particle injection locations.	37
30. Grass height gage showing uncut grass to be about an average of 3.25 inches....	38
31. Grass height gage showing cut grass to be about an average of 2.25 inches.....	38
32. Particle velocity monitoring location.....	40
33. Observation locations for material buildup and dispersion.	40
34. Beginning stages of material buildup in the B1 model discharge chute.....	41
35. B1 model DEM snapshot showing particle streams into the discharge chute and the material dispersion at the back of the hopper.	42
36. Beginning stages of material buildup in the B2 model discharge chute.....	43
37. B2 model DEM snapshot showing particle streams into the discharge chute and the material dispersion at the back of the hopper.	43
38. Beginning stages of material buildup in the Iter1 model lower chute, left.....	44
39. Iter1 model DEM snapshot showing particle streams into the discharge chute and the material dispersion at the back of the hopper.	45
40. Beginning stages of material buildup on the Iter2 model winkle picker.	46
41. Iter2 DEM snapshot showing particle streams into the discharge chute and the material dispersion at the back of the hopper.	46

42. Number of tests run in each grass type.	48
43. Number of tests run in each grass height.	49
44. Number of tests run at each height of cut.	50
45. Graphical view of DEM data points of average particle velocity at the MCS chute exit for each model.....	51
46. CFD cross-section results compared side by side.	56
47. Lift component of velocity above the HoC.....	59
48. Average pressure sampled in the hopper.	60
49. Parametric “de-featuring” of the mower deck shell.....	61
50. CFD bounding box and mower blade control volumes.	62

LIST OF TABLES

Table	Page
1. Variable and variable types.....	5
2. Baseline 1 CFD and test data flow field cross-section velocities.	29
3. Baseline 2 CFD and test data flow field cross-section velocities.	30
4. Iteration 1 CFD and test data flow field cross-section velocities.	31
5. Iteration 2 CFD and test data flow field cross-section velocities.	33
6. Average particle velocity at the MCS chute exit for each model.	51
7. Model information.	55
8. Percentage breakdown of number of tests conducted in each grass type.	57
9. Percentage breakdown of number of tests conducted at each height of cut.	57
10. Percentage breakdown of number of tests conducted in each grass height.	58

ACKNOWLEDGEMENTS

I would first like to thank my advisor, Dr. Marcellin Zahui, for his guidance and support throughout my time as a student at the University of North Dakota. I would also like to give a special thanks to my wife, Jessica, for her support and understanding throughout my graduate career.

This research project was supported by John Deere Horicon Works. I would like to thank Eugene Hayes, Brian Cisar, the rest of the Select Series Team, and the CFD/DEM team who have helped me throughout this project. I must also thank Deere & Company for support of my continued education.

To my two children: Kinley & Lincoln.

ABSTRACT

This thesis will focus on rear discharge bagging performance for Rear Discharge Rear Collect (RDRC), Select Series Lawn & Garden tractors. The problem under investigation pertains to adequately transporting cut grass from the mower deck to the dedicated hopper, without the plugging of the rear discharge chute or the deck mounted chute. The most problematic weather related factors are dew and rain, with the former being the most severe. Conditions creating this problem typically occur during the spring months and when the grass is at its healthiest state.

Field research and data have been collected to gain a better understanding of any and all factors involved as well as what factors can be controlled, what factors are uncontrollable, and what factors can be held constant. Computational Fluid Dynamics (CFD) and Discrete Element Method (DEM) simulations have been conducted to aid in geometry factor identification, field data validation, and field performance predictions.

During this study, a path was identified that leveraged the airflow generated by the mower blades through the rear discharge and mower deck chutes, in moving cut grass from the mower deck to the hopper. Further development of the chutes airflow has aided in increased bagging performance and decreased plugging during tough mowing conditions. Consequently, a better understanding of the CFD and DEM models result in improvements to future model analyses.

CHAPTER I

INTRODUCTION

Description of Project

The first John Deere RDRC tractor was produced in the late 1990's. Since then several more RDRC model line-ups have gone into production. In reality, the development of the “ultimate bagging machine” has been going on for some time. With recent advancements in technology – both CFD and DEM – we have been able to utilize these design tools to aid in the development of bagging performance.

Bagging performance is a term used to describe how well or poor a tractor can transport grass from the mower deck to a hopper. It is essential for RDRC tractors to perform with a high level of bagging performance. Without it, a user's productivity decreases, by spending time unclogging chutes instead of mowing. This frustrates customers because the machine does not adequately perform its primary function. Other mowing modes – mulching and rear discharging – must come secondary to bagging, but should not be ignored. These modes should be monitored to ensure that steps are taken to mitigate any adverse side effects due to the increase of bagging performance. One other thing that should be monitored, not ignored, during bagging performance development is something referred to as cut quality. Cut quality refers to how well the mower deck does at producing a good looking cut.

Engineering field tests were developed to help drive differences between different geometry configurations and determine what conditions are the toughest to bag. It was very apparent early on that weather and grass conditions were large factors in bagging performance, both being virtually uncontrollable variables. What could be somewhat controlled was the time at which field tests were conducted. Field data has been collected on several fronts to aid in the development and correlation of what is seen in the field versus the virtual CFD and DEM models.

Although there are a variety of RDRC machines within John Deere, the RDRC residential unit referenced in this paper can be seen in Figure 1.



Figure 1. CAD model of the John Deere Select Series X350R Model Year 16 Tractor. This is a typical looking dedicated RDRC unit.

Need for Project

The need for this project started in the fall of 2013, when development and field testing of current design practices for RDRC tractors was met with less than satisfactory success in certain bagging conditions. As previously mentioned, weather has a very large impact on bagging performance. During field testing, it was found that healthy grass, mixed with the right weather conditions – moderate to large moisture contents – yielded unfavorable results.

It was at this time that the decision was made to reevaluate the definition bagging performance and determine what could be done to improve performance in the above mentioned corner condition. First, factors were identified that play a role in bagging performance, which of these factors were controllable and which were uncontrollable. Next, theories were developed based on previous experience and existing models. Finally, a determination on how to gather test data for correlation between engineering field tests and virtual testing was needed in order to validate theories, and ultimately improve the bagging performance of the machine.

Similar External Projects

In 2003, two people from the University of Wisconsin-Milwaukee, W. Chon and R.S. Amano, produced an article that was featured in the International Journal of Rotating Machinery, called “Investigation of Flow Behavior around Corotating Blades in a Double-Spindle Lawn Mower Deck” [1]. This paper includes not only a virtual model of a mower deck but also a lab test setup and procedure for conducting indoor testing to correlate CFD to the physical model.

Also, in an online forum at lawnsite.com [2], a lab test fixture from Husqvarna was shown with a small description on how they correlate CFD to the physical model for a mower deck. Husqvarna's Combi deck is in the picture and description posted.

In both of the above instances, there could be something to learn for developing a lab test setup to better correlate CFD to physical models. It must be stated however, that both of these instances were done only on mower decks, not on a complete material collection system.

CHAPTER II

VARIABLE IDENTIFICATION

Introduction

A broad look at the variables that affect bagging performance, both directly and indirectly, will be reviewed in this chapter. There are three primary variable categories; Nature, Natural, and Design. A list of variables can be seen in Table 1 below.

Table 1. Variable and variable types.

Variable	Variable Type	
Moisture	Nature	Uncontrollable
Temperature	Nature	Uncontrollable
Wind	Nature	Uncontrollable
Grass Type	Natural	Controlled
Grass Moisture Content	Natural	Uncontrollable
Grass Height	Natural	Controlled
Grass Health	Natural	Uncontrollable
Deck Shell Geometry	Design - Mower Deck	Constant
Deck Chute Geometry	Design - Mower Deck	Variable
Blade Design	Design - Mower Deck	J-Wing
Blade Speed	Design - Mower Deck	2,850 RPM Nominal
Winkle Picker	Design - Mower Deck	Variable
Deck Rake	Design - Mower Deck	6 MM -10 MM
Deck Baffles	Design - Mower Deck	Variable
Vane	Design - Mower Deck	Variable
MCS Chute Geometry	Design - MCS	Variable
Hopper Bag Material	Design - MCS	Polypropylene Knit
Back Plate Venting	Design - MCS	Variable
Cut Height	Design - External	1 IN - 4.25 IN
Machine Ground Speed	Design - External	Variable
Engine Specs	Design – External	3,100 RPM/18.5 HP Nominal

Nature Variables

All nature variables are virtually uncontrollable with respect to bagging performance. There is one primary weather related item and two secondary items that will be considered as nature variables. They all have strong relationships and are either directly proportional or indirectly proportional. The primary variable is moisture. And moisture can come in two forms, dew or rain. The two secondary variables are temperature and wind.

To give a mental picture, consider a typical day between the sunrise of one day, to the sunrise of the next. And for the purpose of this discussion, the season is spring – where grass is healthiest. Mornings are usually cool and damp with little to no wind. As the day progresses, temperature rises and moisture decreases, with wind speeds picking up. As the day comes to a close, temperature and wind speeds decrease, while moisture increases throughout the night.

Temperature and wind directly affect grass moisture content, both internally and externally. A typical morning with good weather conditions for testing produces moisture on the grass. An early morning view of the test field with good weather conditions can be seen in Figure 2 below.



Figure 2. Early morning testing weather conditions at the cut plots. Overcast sky, dense fog, and mist (external grass moisture).

Natural Variables

For the purpose of this discussion, natural variables will be related to the grass or grass condition. Natural variables do not have strong relationships with one another but are very dependent on the nature variables previously mentioned. The four main natural variables are grass type (dependent on locale), internal grass moisture content, grass health, and grass height (or length).

Grass type is dependent on climate with the most common ones tested being Rye, Blue Grass, and Fescue. Grass moisture content is dependent on the season, typically having its highest moisture retention in the spring. Grass health has several components

and is somewhat subjective under viewing. For example; grass density, weed content, and the amount of underlying thatch or dead grass all make up grass health. Grass height is very dependent on the season and thusly sun and moisture. Grass types and grass heights will be considered controlled during engineering field tests.

Design Variables

Design variables can be broken up into three categories; mower deck variables, MCS variables, and external design variables. Many of the design variables listed in Table 1 can and were able to be held at constant values. Even though development continually drives changes in design, a typical RDRC setup has the following basic components, identified in Figure 3.

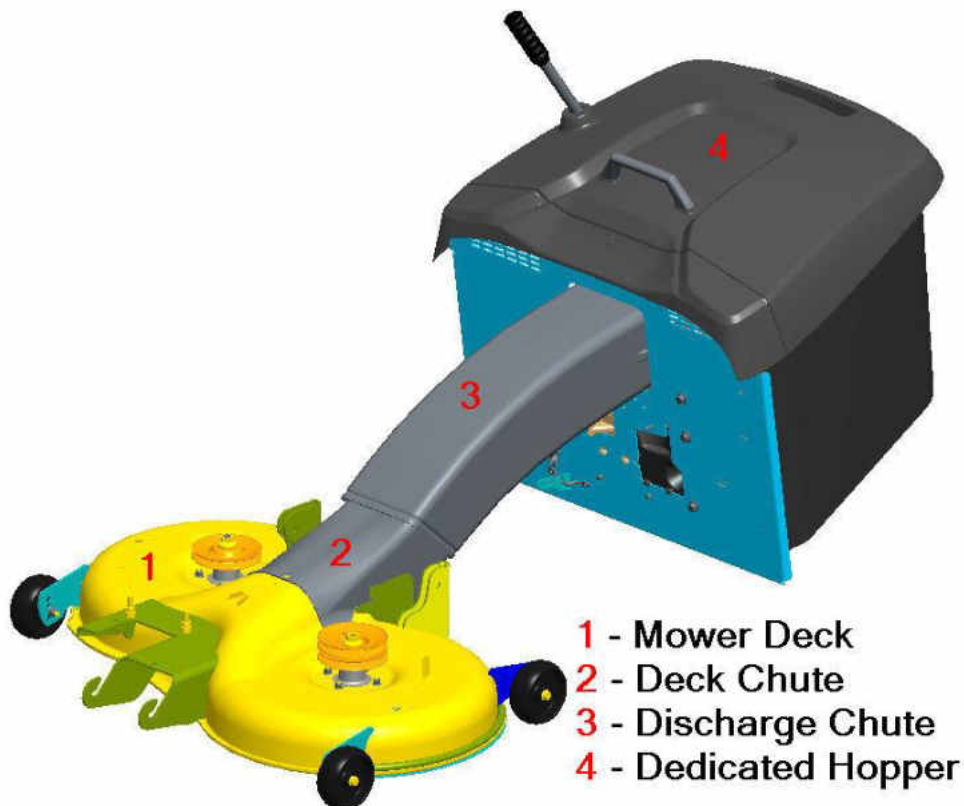


Figure 3. CAD model of the X350R Material Collection System.

Mower Deck Variables

Deck shell geometry was held constant for testing. Deck chute geometry was developed throughout virtual and engineering field tests. Deck chute geometry dictates attack angle and is important for the initial direction of airflow and launch direction of particles. Deck shell and deck chute geometry can be seen in Figure 4 and Figure 5. Attack angle and deck rake can be seen in Figure 5. Deck rake is the height difference between the front of the deck shell versus the rear of the deck shell and allows for additional airflow into the mower deck.



Figure 4. Deck shell and deck chute geometries. 1) Deck shell. 2) Deck chute.

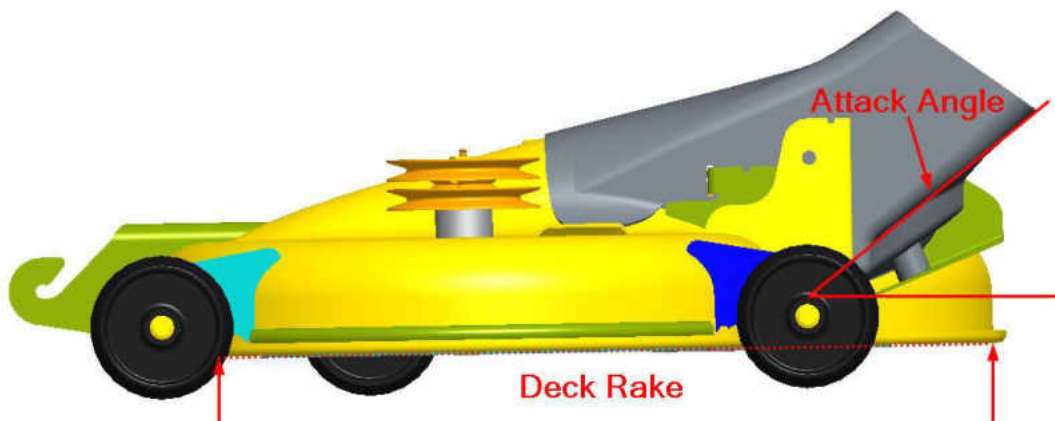


Figure 5. Attack angle and deck rake.

A J-wing blade design with a 33mm wing height and a 115mm wing length was used for official testing. Blade speeds were held constant at a nominal of 2,850 revolutions per minute for official testing. Some experimenting was done to validate design direction taken. Blade designs can be seen in Figure 6.

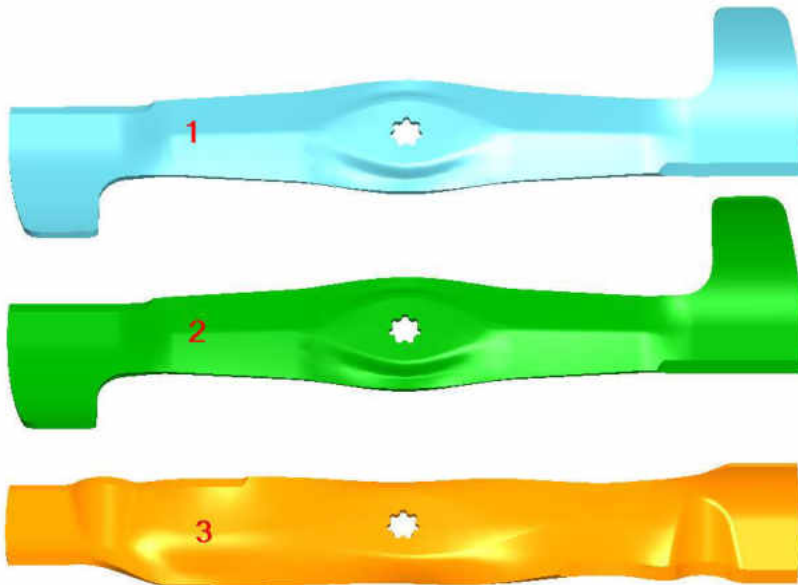


Figure 6. Mower blade designs. 1) J-wing design with a 33mm wing height and a 115mm wing length. Used in virtual and engineering field tests. 2) J-wing design with a 43mm wing height and a 115mm wing length. 3) 3-n-1 blade design with a 33mm wing height and a 76mm wing length.

In the underside view of the deck in Figure 7, you can see the winkle picker, vane, and connecting v-baffle. The winkle picker is a protrusion from the back of the mower deck that extends up to the left and right blade tangency, directing air and particle flow up the lower chute.

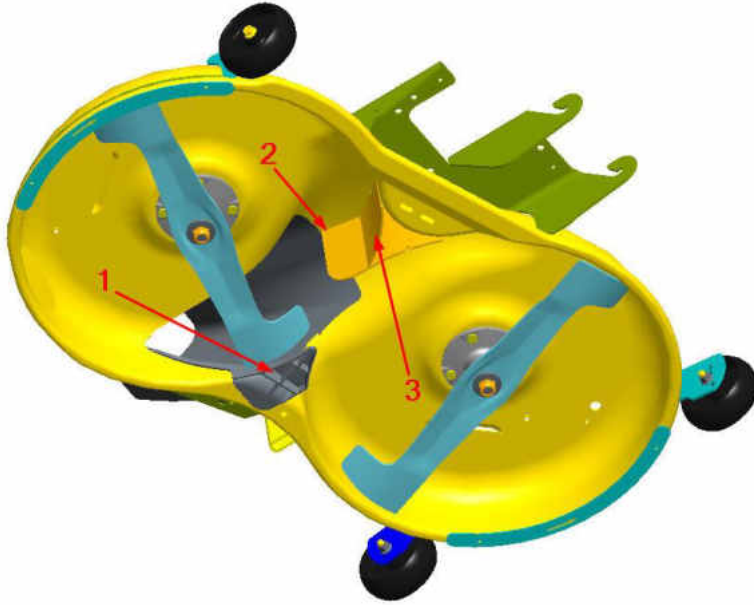


Figure 7. Underside view of mower deck. 1) Winkle picker. 2) Vane. 3) V-baffle.

Material Collection System Variables

The goal of the MCS chute is to gently guide air and particles into the hopper, not forcibly direct flow movement. Flow direction should happen as close to the mower blades as possible and therefore occurs at the lower chute. Hopper bag material will be considered a constant throughout this discussion and should adequately retain particles while allowing as much breathing capability as possible to reduce hopper back pressures. Polypropylene knit was used for hopper bag material and a single layer of polyester was used for the dust curtain throughout all of engineering testing. Volume of the hopper was held constant at 270 liters. Back plate venting also aids in reducing hopper back pressures. The MCS design variables can be seen in Figure 8.

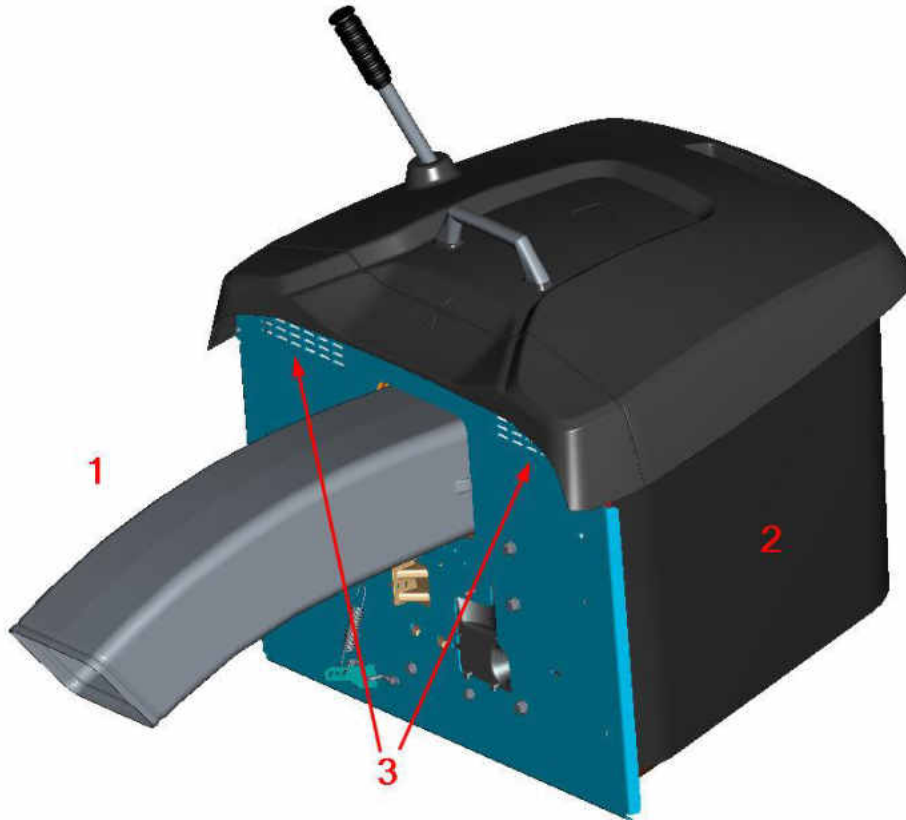


Figure 8. Material Collection System Design Variables. 1) MCS chute. 2) Hopper bag. 3) Back plate venting.

External Variables

For the purpose of this discussion, engine specs will be considered constant throughout testing. Engine specs can influence bagging performance, horsepower and torque as well as carbureted or electronically controlled, play a role in how well blade speed can be maintained throughout the many various grass conditions. Ground speed also plays an important role, the faster a machine travels the less time a blade has to cut grass before being introduced to more uncut grass. In other words, the amount of grass being processed increases as speed increases. Ground speeds varied during engineering tests and were largely dependent on the processing capability of the unit at that time. Cut

height (also referred to as height of cut or HoC) is another important factor. As grass height increases and HoC decreases, material being processed increases. HoC varied during field particle testing to allow for different amounts of grass to be processed and drive differentiation between test models. For field airflow tests and all virtual testing, HoC was held constant at 3.25 inches.

Summary

In summary, the toughest bagging condition exists when grass is healthy, retains large amounts of moisture, and the external moisture content is high. Material being processed increases during any of the following events; a grass height increase, a HoC decrease, a ground speed increase, and an internal or external moisture content increase. The primary design variables considered are the deck and MCS chutes.

CHAPTER III

TEST MODELS

Introduction

The four models described below were tested virtually. CAD software used for model generation was PTC Creo Parametric, version 2.0 from PTC Incorporated [3]. The CFD software used was Star CCM+, version 9.04.009 from CD-adapco and the DEM software used was EDEM, version 2.6 from DEM Solutions [4], [5]. Field operation was also observed and data collected to aid in model correlation. All models had a V-baffle, used J-Wing mower blades and were designed for nominal blade speeds of 2,850 revolutions per minute. The mower deck shell geometry, hopper size and hopper bag material stayed constant through testing. The vertical travel of the mower deck in each of the below models is 1 inch to 4.25 inches above the ground plane.

Baseline 1

The initial or baseline 1 model (B1) was centered on making the discharge chute as large as possible throughout the existing design space. This was done in an attempt to accommodate as much material flow through the chute as possible. The discharge chute was fixed and the lower chute was flexible – spring hinged. The back plate venting open area in B1 is 39,600 square millimeters. An overview of the B1 design can be seen in Figure 9 below.

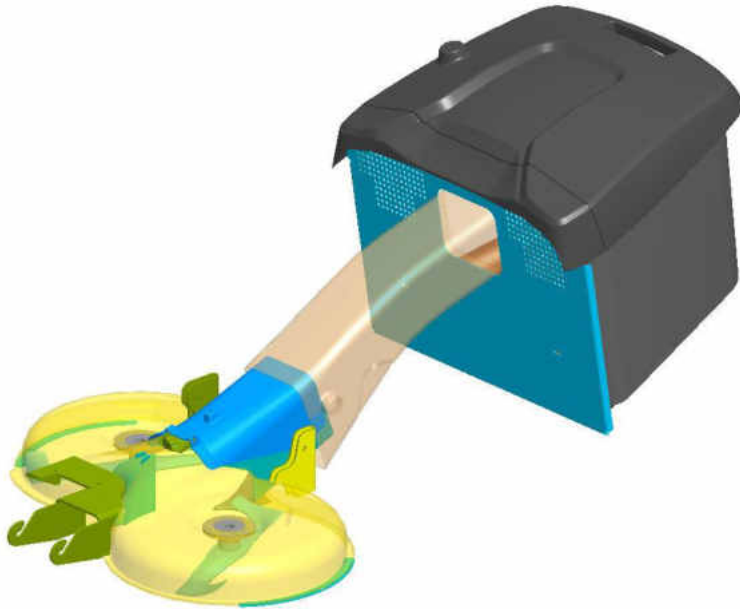


Figure 9. CAD model of the B1 design.

Below, Figure 10 shows a cross-section view of the B1 model, 70 millimeters left of centerline with the mower blades 3.25 inches above the ground plane. In this figure you can see the top portion of the deck chute contacting the top of the MCS chute while a gap is created between the bottom of the deck chute and the bottom of the MCS chute. At a 1 inch HoC the gap is 0.0 millimeters and at 4.25 inch HoC the gap created is 50 millimeters.

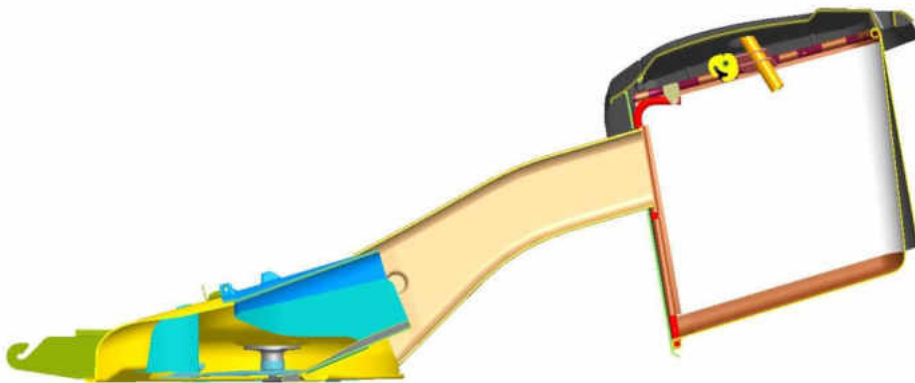


Figure 10. Cross-section view of the B1 model. Located 70 millimeters to the left of centerline with the blades at a 3.25 inch HoC. Deck to MCS chute gap is 35 millimeters.

The deck chute attack angle is 22 degrees from horizontal in the B1 model. The deck and MCS chute exit areas are 34,700 and 36,700 square millimeters, respectively, giving a chute exit ratio of 1.06. As can be seen in the above figure, there is a V-baffle and a winkle picker, but no vane. The deck is raked 6 millimeters in this model.

Baseline 2

The baseline 2 model (B2) was centered on making the discharge chute flexible and the deck chute fixed to the deck in the same design space as B1. This was done in an attempt to prevent changes to the surrounding functional groups. The discharge chute is retained at the back plate and allowed to pivot. The back plate venting open area in B2 is 39,600 square millimeters. An overview of the B2 model can be seen in Figure 11 below.

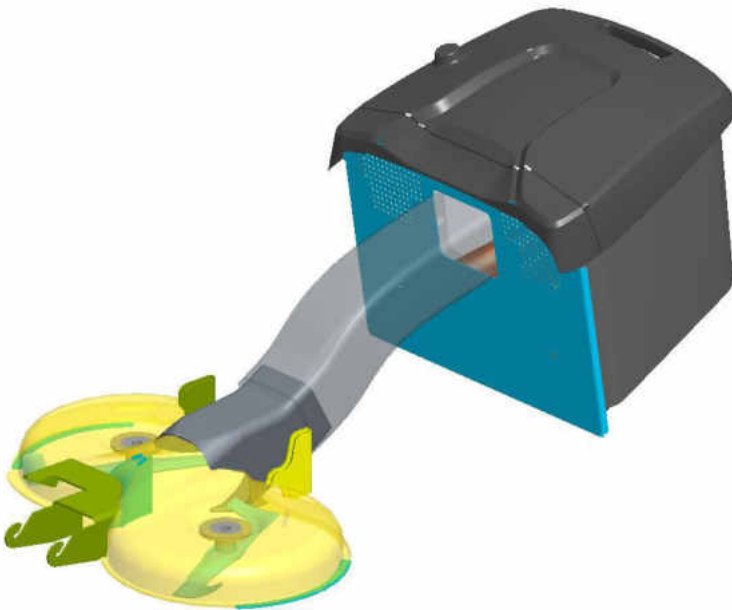


Figure 11. CAD model of the B2 design.

Below, Figure 12 shows a cross-section view of the B2 model, 70 millimeters left of centerline with the mower blades 3.25 inches above the ground plane. In this figure

you can see the gap between the deck and discharge chute was removed. As the deck is raised and lowered, the lower chute telescopes inside the discharge chute. To avoid changing of other functional groups, an “S” shape was created in the design of the discharge chute.

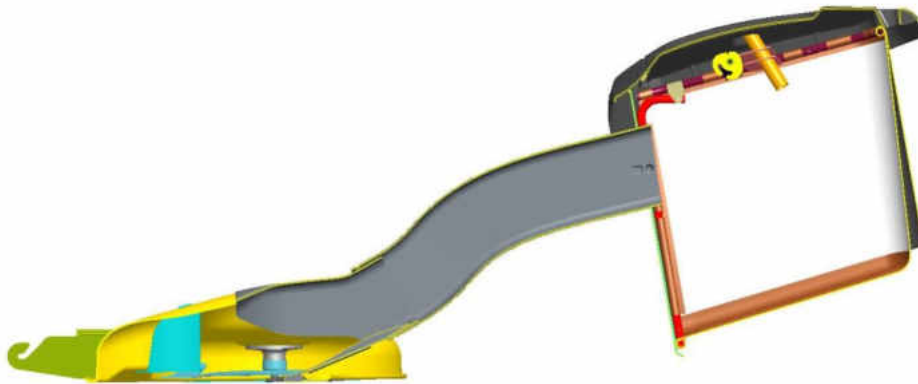


Figure 12. Cross-section view of the B2 model. Located 70 millimeters to the left of centerline with the blades at a 3.25 inch HoC.

The deck chute attack angle is 28 degrees from horizontal in the B2 model. The deck and MCS chute exit areas are 31,600 and 39,700 square millimeters, respectively, giving a chute exit ratio of 1.26. As can be seen in the above figure, there is a V-baffle and a winkle picker, but no vane. The deck is raked 6 millimeters in this model.

Iteration 1

The first iteration model (Iter1) was centered on redesigning the MCS design space which required design changes in multiple functional groups. The new design space put the lower chute at forefront of performance variables where in past designs it has been the MCS chute. The discharge chute is retained at the back plate and allowed to pivot. The back plate venting open area in Iter1 is 21,600 square millimeters. An overview of the Iter1 design can be seen in Figure 13 below.

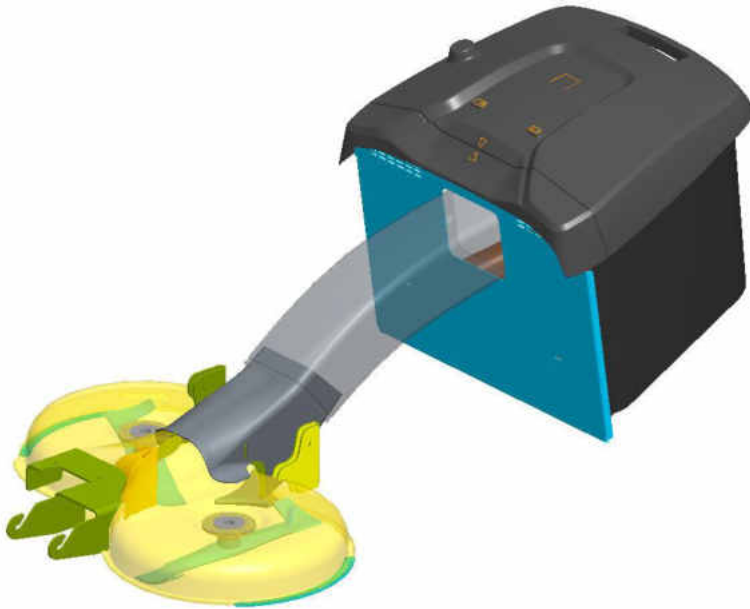


Figure 13. CAD model of the Iter1 design.

Below, Figure 14 shows a cross-section view of the Iter1 model, 70 millimeters left of centerline with the mower blades 3.25 inches above the ground plane. As can be seen in this figure, the “S” was removed from the MCS chute and replaced by an arc rearward to the hopper. The deck chute was significantly modified for Iter1 to immediately direct flow of particles and air more upwards than past designs. The telescoping of the two chutes was retained from the B2 design.

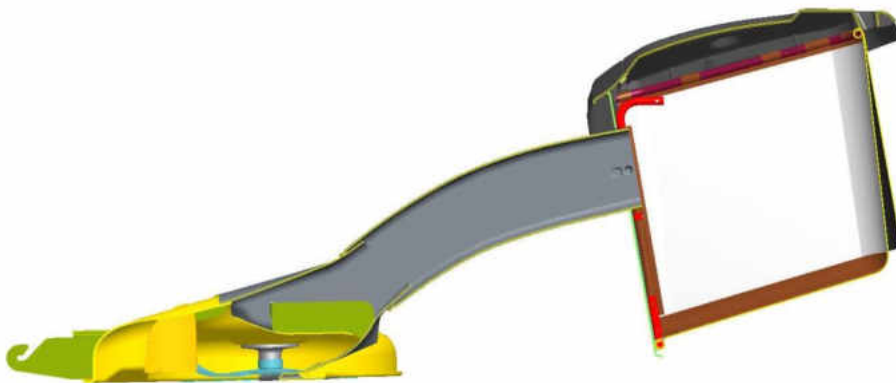


Figure 14. Cross-section view of the Iter1 model. Located 70 millimeters to the left of centerline with the blades at a 3.25 inch HoC.

The deck chute attack angle is 43 degrees from horizontal in the Iter1 model. The deck and MCS chute exit areas are 29,700 and 38,700 square millimeters, respectively, giving a chute exit ratio of 1.31. As can be seen in the above figure, there is a V-baffle, a winkle picker, and a small vane. The deck is raked 10 millimeters in this model.

Iteration 2

The second iteration model (Iter2) focused on optimizing performance through small design changes based on experiences and findings from past designs. The discharge chute continued to be retained at the back plate and allowed to pivot. The back plate venting open area in Iter2 is 21,600 square millimeters. An overview of the Iter2 design can be seen in Figure 15 below.

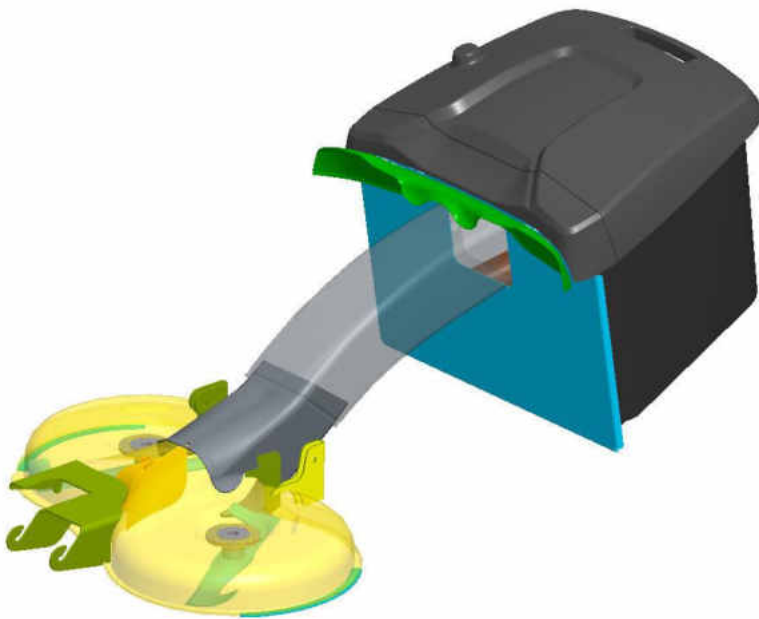


Figure 15. CAD model of the Iter2 design.

Figure 16 below shows a cross-section view of the Iter2 model, 70 millimeters left of centerline with the mower blades 3.25 inches above the ground plane. As can be seen

in this figure, the lower portion of the deck chute was straightened and the curvature of the discharge chute was reduced compared to the Iter1 design. The telescoping of the two chutes was retained from the B2 design.

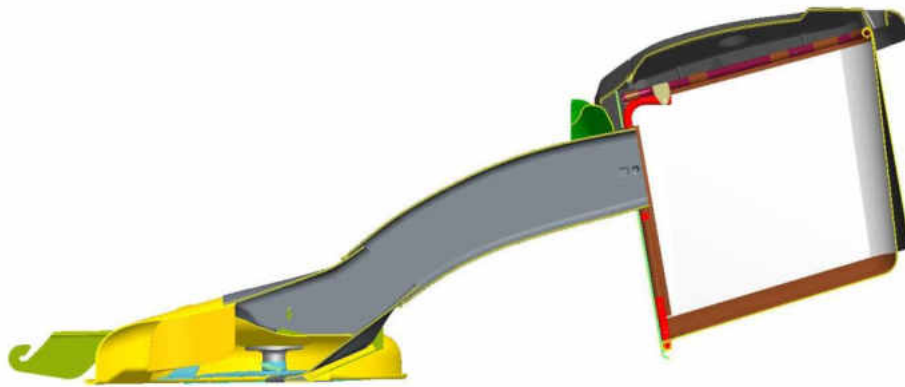


Figure 16. Cross-section view of the Iter2 model. Located 70 millimeters to the left of centerline with the blades at a 3.25 inch HoC.

The deck chute attack angle is 38 degrees from horizontal in the Iter2 model. The deck and MCS chute exit areas are 30,500 and 38,300 square millimeters, respectively, giving a chute exit ratio of 1.26. In the above figure, the vane was enlarged and integrated with the V-baffle. The winkle picker was retained and the deck was raked 10 millimeters in this model.

CHAPTER IV

AIRFLOW TESTING OVERVIEW

Theory Development

With B1's deck chute being flexible, this caused the deck chute exit to vary with cut height. Consequently, this changed the flow characteristics at the deck chute exit and throughout the MCS chute. Little was known about the airflow characteristics and particle interactions imparted by the mower blades at this time. A virtual analysis was conducted and field data was collected on the B1 model to better understand the airflow and particle interactions throughout the chutes. This data collection quickly showed that airflow played a much more important role than previously known. The following was theorized. - Velocities at the lower chute should be higher than the exit of the discharge chute. -

A new baseline was created (B2) that incorporated the above theory. With the lower chute being changed from flexible to fixed, this allowed a constant lower chute exit cross section at all heights of cut. In turn, it also allowed the lower chute to be necked down, creating a nozzle, giving more control to air speed at the lower chute exit over the range of cut heights. Virtual analysis and field data for B2 was collected giving insight to airflow for the previously mentioned theory. The theory was validated but amended due to new information. - Airflow should be immediately directed by the lower chute into the

discharge chute. Velocities at the lower chute exit should be higher than the exit of the discharge chute. The discharge chute should act as a guide, not forcibly directing airflow.

- This has been the theory that Iter1 and Iter2 have been modeled to and operated under.

Test Setup

Field

For flow data collected in the field, the test setup consisted of very few components. First, tires need to be pressurized to the correct operating pressure. In all test cases, tire pressure was the same. The front tires were inflated to 14 pounds per square inch and the rear tires were inflated to 10 pounds per square inch. Second, the mower deck needs to be leveled and the correct rake induced. The deck leveling gage can be seen in Figure 17.

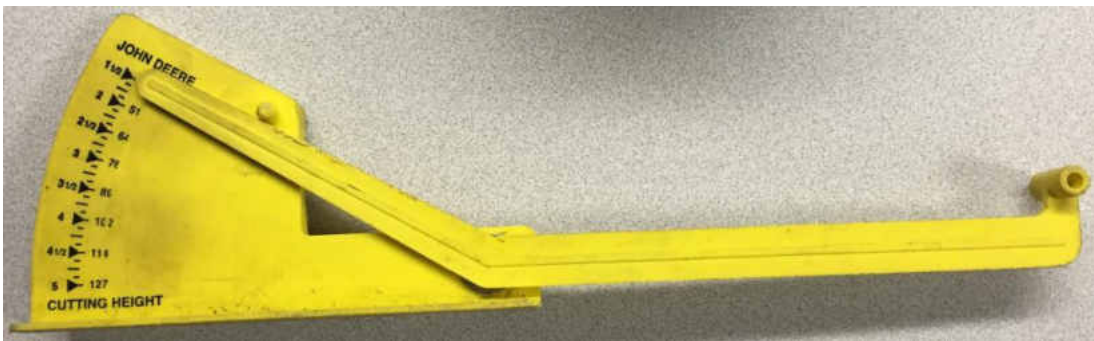


Figure 17. Mower deck leveling gage. Has a range of 1.5 – 5.0 inches.

Third, three small access holes for the digital manometer need to be drilled in the MCS chute near the chute exit and three more holes in the MCS chute near the lower chute exit. The three holes allowed for a 3x3 grid of measurements to be taken. The two cross-sections were chosen to measure flow at the nozzle of the lower chute and as far

away from the mower deck as geometry would allow. The two cross-sections can be seen in Figure 18.

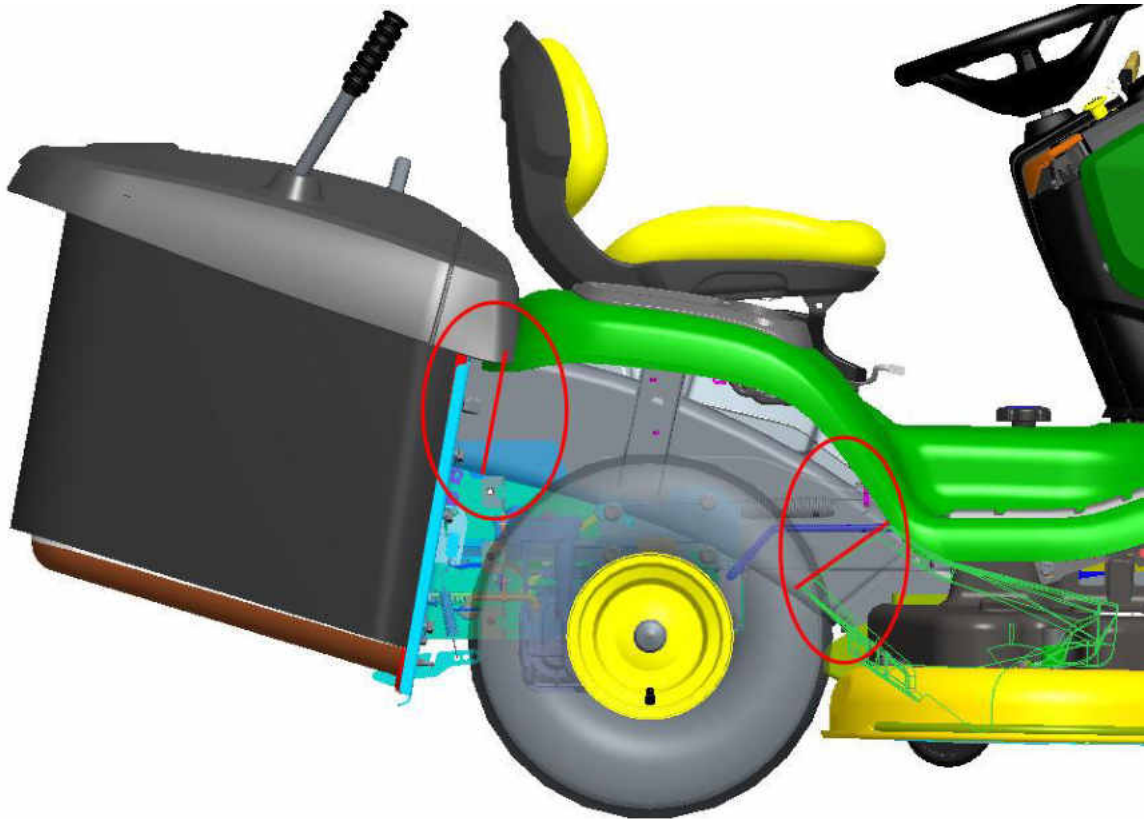


Figure 18. Flow measurement locations. Grid measurements were taken near the lower chute nozzle and near the MCS chute exit.

Fourth, the digital manometer needs to be zeroed. The digital manometer used for taking field measurements can be seen in Figure 19. Equations for converting pressures to velocities as well as examples and general guides for using the digital manometer were taken from the Dwyer Instruments, Inc. website on their Air Velocity Measurement page [6].



Figure 19. Dwyer Instruments, Series 475 Mark 3 Digital Manometer. This manometer has a range of 0 – 10.00 Inches of W.C. (water column) or 0 – 2.49 kPa.

Virtual

Prior to any CFD analyses, a pressure drop study needed to be conducted on the two types of polypropylene knit that makes up the hopper bag. Flow versus pressure drop data was collected on these two materials. These pressure drop characteristics were applied to the hopper bag in the CFD analyses. The curves generated can be seen in Figure 20.

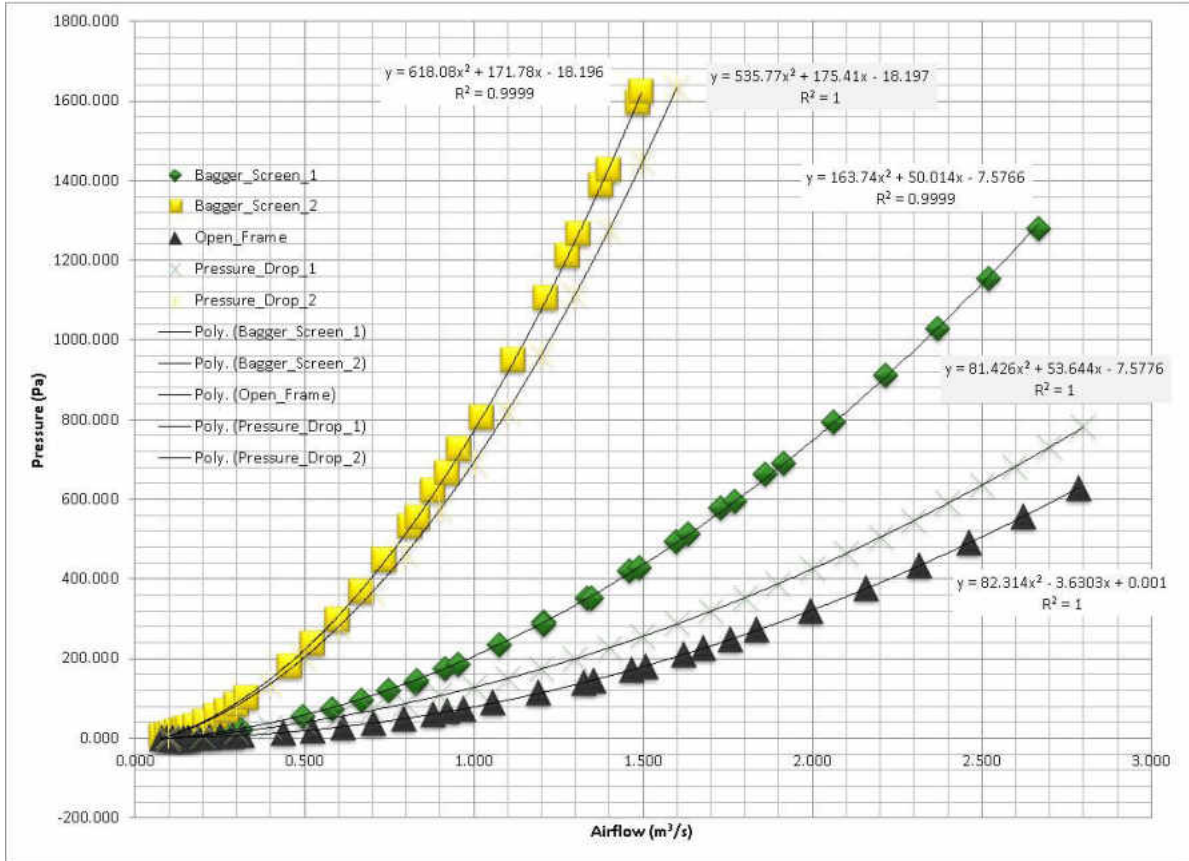


Figure 20. Flow versus pressure drop of the hopper bag materials.

Small simplifications; such as the removal of fasteners, removal of fastener holes, and filling-in of small gaps between parts, was done to the geometry models for the virtual analysis. These simplifications helped reduce CFD and DEM setup and computation times.

Numerous inputs were held constant through each CFD analysis. Such as; blade speeds of 2,850 revolutions per minute, a cut height of 3.25 inches, wind speed of 0 miles per hour, and air temperature of 22 degrees Celsius. The hopper was also assumed to be clean and empty for each analysis. The CFD domain size was 3 meters by 2 meters by 3 meters, in the X (width), Y (height), and Z (length) directions.

Test Method

Field

Nine data points were taken at each of the two cross-sections for each model, shown in Figure 21.

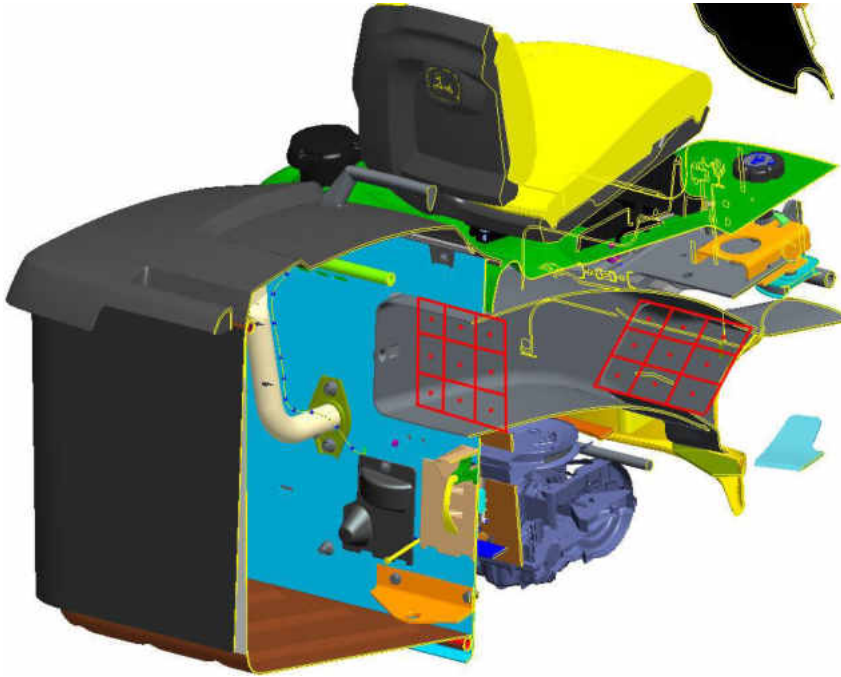


Figure 21. Air data measurement locations taken in the field. Nine data points at each cross-section, two cross-sections per model.

The following procedure was used for each of the eighteen data points taken inside the MCS chute for each of the four test models:

- Inserted Pitot tube through access hole in the chute and aligned to be parallel to flow direction.
- With tractor at high idle, the mower deck was engaged.
- With blade speed at steady-state, pressure measurements were monitored by two people over a three second time interval.

- The average of the two reported numbers was recorded.

Virtual

The locations for field data collection were also mapped virtually to view the flow field during CFD. The same nine data points were averaged and recorded at each cross-section, for each model, after the transient airflow in the system reached “steady state”.

The cross-section locations shown in Figure 22, were used for all test models.



Figure 22. CFD flow field locations within the MCS chute. The one on the left being the deck chute nozzle exit and the one on the right being near the exit of the MCS chute.

Results – Field & Virtual

The results for each model have been color coded to show flow field intensities at each cross-section. For simplicity and side-by-side comparison, each model is shown in a table format, with CFD results on the left and test data on the right. All velocities are reported in meters per second. The full CFD contour plots can be viewed in Appendix B.

Baseline 1

As previously mentioned about the B1 design, there is a gap created as cut height increases between the lower portions of the deck chute and MCS chute. It was observed both in CFD and in the field that airflow would make a 180 degree turn and exit the chute

through this gap. Figure 23 shows this wake region as well as a small wake region just past the top of the deck chute in the MCS chute.

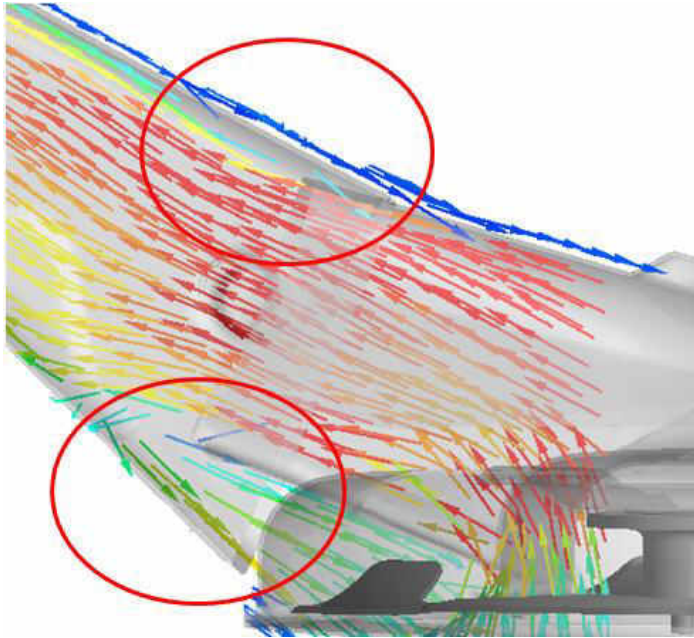


Figure 23. Wake regions generated in the Baseline 1 CFD model.

The B1 flow field results can be seen below in Table 2. The colored results displayed show higher velocities exist at the top and left portions of the deck chute nozzle, where the higher velocities near the exit of the MCS chute are primarily left and center. This showed a twisting of high velocity airflow throughout the MCS chute. The CFD average cross-section velocities for the nozzle and MCS chute are 20.5 and 18.6 meters per second, respectively. The test data average cross-section velocities for the nozzle and MCS chute are 18.0 and 17.3 meters per second, respectively.

Table 2. Baseline 1 CFD and test data flow field cross-section velocities.

		Baseline 1						
		CFD (m/s)			Test Data (m/s)			
Nozzle		24.0	23.0	22.0	22.3	18.8	21.3	Nozzle
		23.0	20.0	21.3	18.9	15.7	17.4	
		21.0	16.0	14.0	18.5	15.1	14.4	
		CFD (m/s)			Test Data (m/s)			
MCS Chute		21.0	18.5	16.2	19.3	17.0	16.0	MCS Chute
		21.3	18.0	17.8	19.3	17.0	15.1	
		21.2	17.7	16.0	18.6	17.7	15.8	

Baseline 2

Although not a wake region, B2’s unique MCS chute curvature produced a very abrupt velocity reduction of air at the top of the MCS chute after the deck chute exit. The CFD also showed a velocity reduction of air immediately entering the lower portion of the MCS chute. The airflow exiting the lower half of the deck chute was being directed immediately into the bottom curvature of the MCS chute and was being forced to change direction. Figure 24 shows the two velocity reduction regions in the MCS chute.

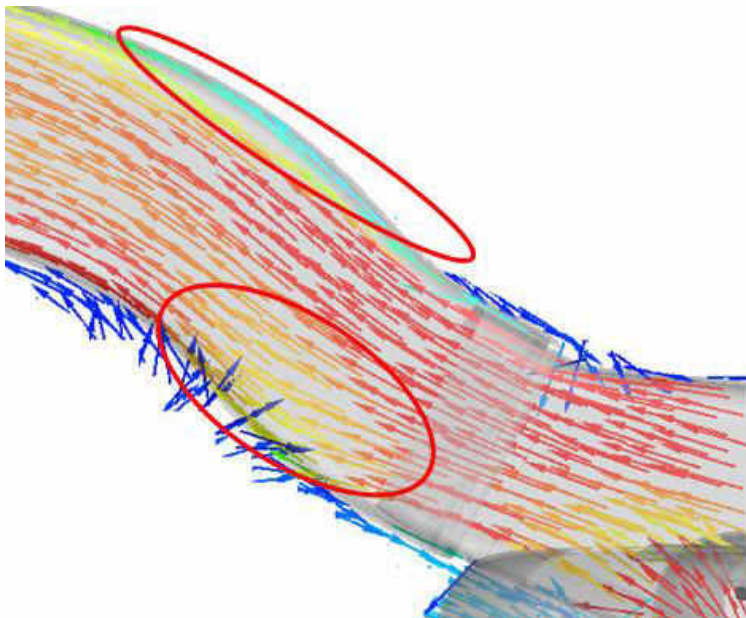


Figure 24. Velocity reduction regions generated in the Baseline 2 CFD model.

The B2 flow field results can be seen below in Table 3. The colored results displayed show higher velocities exist at the top and left portions of the deck chute nozzle, where the higher velocities near the exit of the MCS chute are primarily left and center. Again, this showed a twisting of high velocity airflow throughout the MCS chute, similar to the twist seen in B1. The CFD average cross-section velocities for the nozzle and MCS chute are 20.3 and 17.7 meters per second, respectively. The test data average cross-section velocities for the nozzle and MCS chute are 25.5 and 19.9 meters per second, respectively.

Table 3. Baseline 2 CFD and test data flow field cross-section velocities.

		Baseline 2							
		CFD (m/s)			Test Data (m/s)				
Nozzle		24.0	23.0	22.0	31.5	30.3	30.2	Nozzle	
		22.0	21.0	20.0	28.4	23.9	24.9		
		21.0	16.0	14.0	23.0	20.3	17.0		
MCS Chute		19.0	18.5	16.0	21.1	21.3	20.2	MCS Chute	
		21.2	18.0	15.0	21.4	19.2	17.6		
		20.5	17.5	14.0	21.2	19.6	17.6		

Iteration 1

No wakes were observed in the Iter1 model. Even with the new operating theory, the Iter1 geometry showed an air velocity reduction region in CFD. The location of this region can be seen farther back in the MCS chute in Figure 25 below.

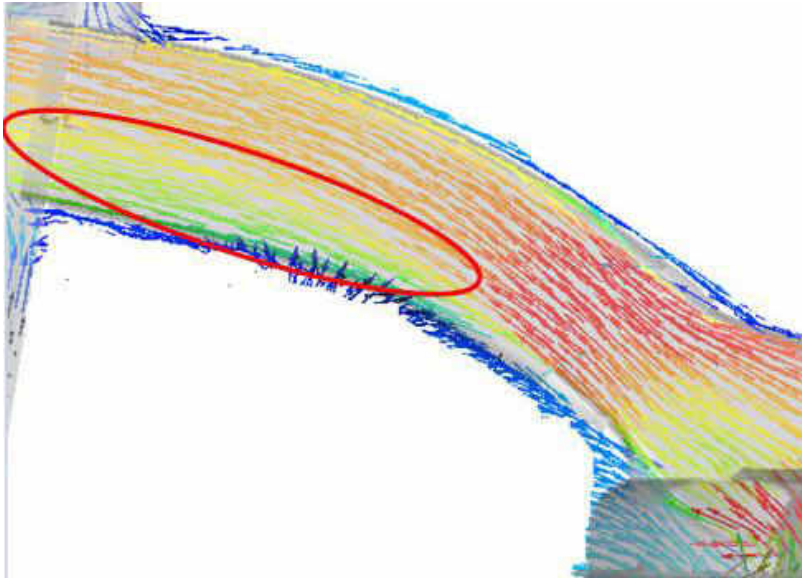


Figure 25. Velocity reduction region generated in the Iteration 1 CFD model.

The Iter1 flow field results can be seen below in Table 4. The colored results displayed show a more even flow from left to right in both CFD and test data; this was attributed to the addition of the small vane inside the deck. The small vane also helped eliminate the twisting of air throughout the MCS chute. Some bias still existed in the upper left portion of the deck chute. The CFD average cross-section velocities for the nozzle and MCS chute are 20.8 and 15.5 meters per second, respectively. The test data average cross-section velocities for the nozzle and MCS chute are 23.4 and 18.6 meters per second, respectively.

Table 4. Iteration 1 CFD and test data flow field cross-section velocities.

		Iteration 1						
		CFD (m/s)			Test Data (m/s)			
Nozzle		22.5	21.3	20.6	26.9	24.1	24.5	Nozzle
		21.8	20.5	21.1	24.5	22.3	21.8	
		19.9	19.7	19.7	24.1	20.8	21.8	
MCS Chute		16.4	17.5	16.4	20.4	19.5	18.8	MCS Chute
		16.0	16.2	16.7	20.9	19.3	18.2	
		12.4	12.7	15.5	18.8	18.4	13.2	

Iteration 2

The Iter2 CFD model showed no wakes throughout the MCS chute. Since Iter2 operated under the same theory as Iter1, a similar air velocity reduction region was observed in CFD. The location of this region can be seen farther back in the MCS chute in Figure 26 below.

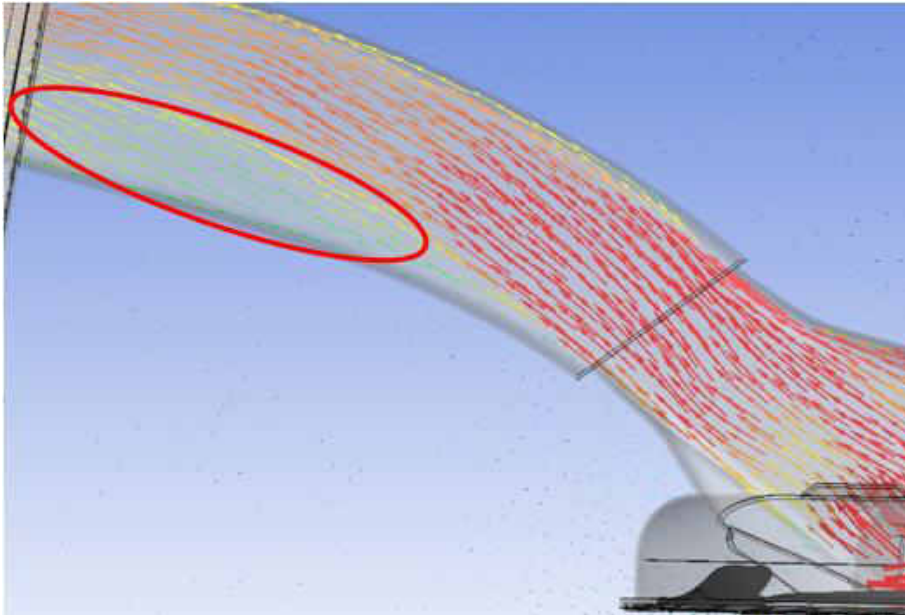


Figure 26. Velocity reduction region generated in the Iteration 2 CFD model.

The Iter2 flow field results can be seen below in Table 5. The colored results displayed show a very evenly distributed flow in the test data. The CFD results showed slightly lower velocities in the center of the chute. The evenly distributed flow from left to right was attributed to the large vane inside the deck as well as the straight-line contour of the lower surface of the deck chute. The large vane also prevented the twisting of air throughout the MCS chute by partially dividing the deck chambers and directing the airflow into the chute. The CFD average cross-section velocities for the nozzle and MCS chute are 23.4 and 18.2 meters per second, respectively. The test data average cross-

section velocities for the nozzle and MCS chute are 23.4 and 18.3 meters per second, respectively.

Table 5. Iteration 2 CFD and test data flow field cross-section velocities.

		Iteration 2						
		CFD (m/s)			Test Data (m/s)			
Nozzle		22.7	23.6	25.4	24.5	23.6	24.9	Nozzle
		25.0	21.3	23.8	23.2	22.7	24.1	
		24.0	21.6	23.5	22.3	22.3	23.2	
		CFD (m/s)			Test Data (m/s)			
MCS Chute		19.4	18.5	17.9	18.2	18.8	19.3	MCS Chute
		18.6	16.3	18.7	18.8	19.3	19.8	
		18.4	15.0	21.0	15.1	17.6	18.2	

Summary

It quickly became apparent through CFD simulations and data collection that controlling airflow early on in the system produced far better results than trying to direct airflow by the MCS chute. Velocity magnitudes could be controlled by lower chute geometry, attack angle, and nozzle size. Airflow distribution could be controlled by the size of the vane used between the left and right deck chambers.

Below, in Figure 27, you can see the progression of velocity magnitudes between models after the chute exit and midway into the hopper. Also below, in Figure 28, you can see the continued progression of velocity magnitudes between models as the air reaches the rear of the hopper. In both of these figures, one can observe the left hand bias of air in the B1 and B2 models. With the added vane and changes in lower chute geometry in the Iter1 and Iter2 models, one can see the increase in velocity magnitudes and a more even flow distribution into the hopper.

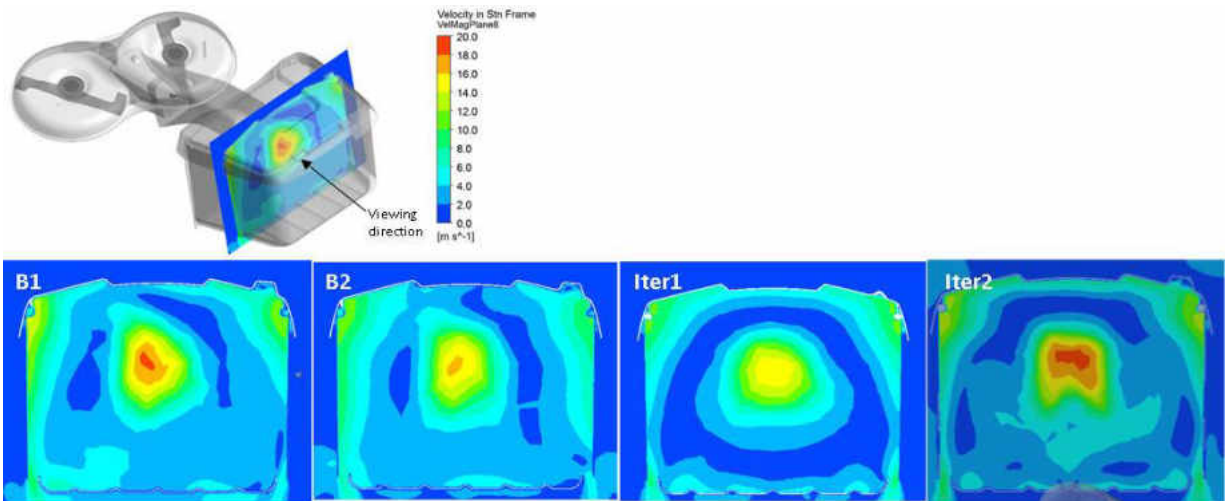


Figure 27. Airflow velocity magnitude midway through the hopper. From left to right: B1, B2, Iter1, Iter2.

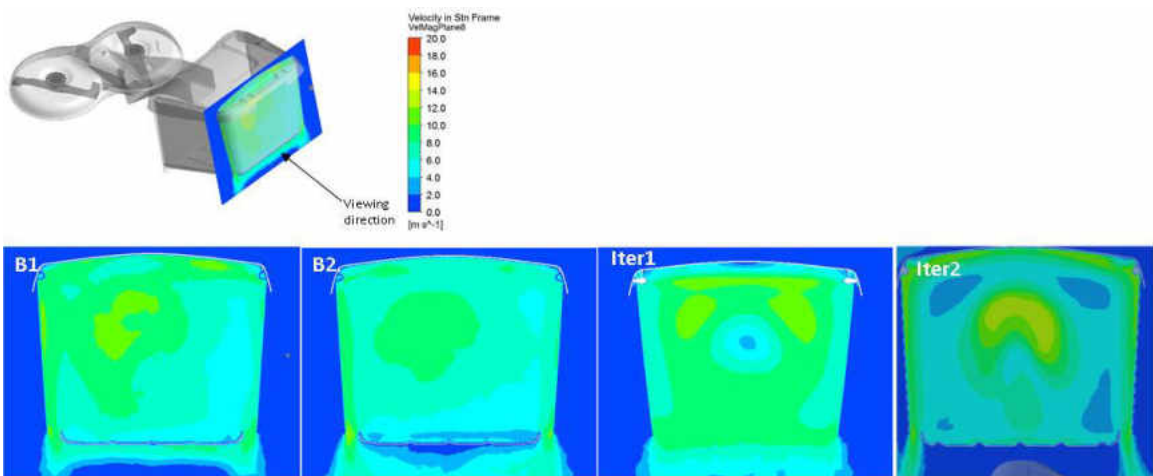


Figure 28. Airflow velocity magnitude at the rear of the hopper. From left to right: B1, B2, Iter1, Iter2.

CHAPTER V

PARTICLE TESTING OVERVIEW

Theory Development

The particle testing theory development paralleled the airflow testing theory development. As previously mentioned, little was known at the time of the B1 model about airflow and particle interactions and the importance of controlling airflow throughout the system. At this time field data was collected and a DEM analysis was conducted on the B1 model. Both gave insight to particle interactions and the following was theorized. - Particles follow high velocity flow streams in the deck chute but fall out of suspension as they approach lower velocity regions in the MCS chute. This is greatly amplified when particles are larger and/or have higher than normal moisture contents. - It was thought that higher velocities would help increase bagging performance.

B2 was created with a nozzle on the deck chute to give a boost to air and particle speeds coming out of the deck. Since the B2 model operated in the same design space as B1, it still maintained a relatively low attack angle of 28 degrees. The curvature of the MCS chute was thought to; direct the air and particle movements. This proved to be false with heavy or high moisture content particle loadings. At this time the following was theorized. - Air and particle flow should be immediately directed by the lower chute into the discharge chute. The attack angle is important for immediate direction of air and

particles from the mower deck. Velocities at the lower chute should be higher than the exit of the discharge chute to aid in initial air and particle trajectories. And the discharge chute should only act as a guide, not forcibly directing air and particle flow. - Two things needed to happen; first, improved airflow distribution throughout the MCS system, and second, immediate influence of air and particles coming from the mower blades. Iter1 and Iter2 were developed from this theory.

Test Setup

Field

Cut plots were maintained before and during field testing. Fertilizer and irrigation systems were used to maintain a healthy, lush grass condition. Maintaining the cut plots also included keeping the grass at desired testing heights, cleaning up clippings after each maintenance session and cleaning up clippings after each test session. Keeping the plots clean from excess clippings helped to reduce thatch and minimized any effects that thatch would have during testing. By maintaining the cut plots in this manner, one is able to somewhat mitigate effects of the variation of grass variables.

Tractor setup for particle testing was done similar to that of the airflow testing. First, tire pressures need to be set, 14 and 10 pounds per square inch for the front and rear tires, respectively. Second, the deck needs to be level from left to right. And third, the correct rake needs to be applied to the mower deck for proper air intake.

Virtual

Multiple grass types were studied and property inputs developed for the DEM simulations. A grass type mixture of Fescue and Rye grass was used in all the DEM simulations. Material properties, grass properties, interaction properties, and grass dimensions were all held constant between each simulation. The simplified CFD geometry models were also carried over into the DEM simulations. The ground was moved at a speed of 5 miles per hour to simulate a machine traveling across the ground and 5,000 particles per second were injected into each chamber at the 12 o'clock position. The particle injection locations can be seen in Figure 29.

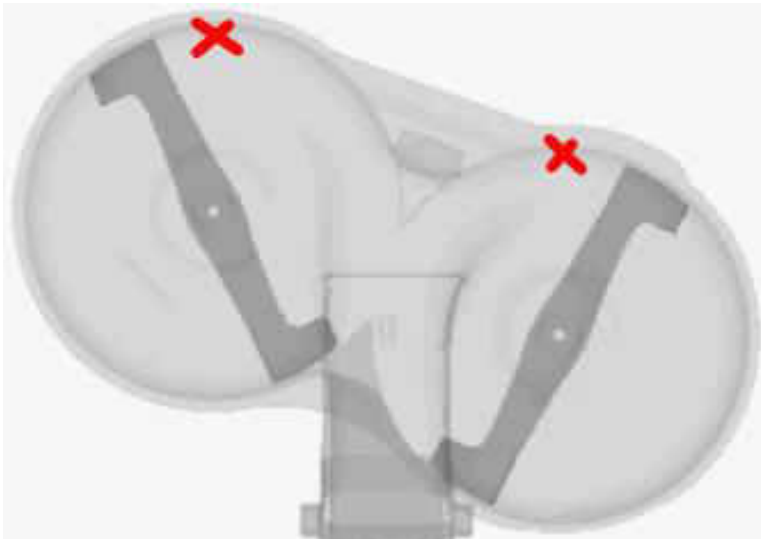


Figure 29. Grass particle injection locations. Two locations, one in each chamber at the 12 o'clock position.

Numerous other inputs were held constant through each DEM simulation. Such as; blade speeds of 2,850 revolutions per minute, cut height of 3.25 inches, wind speed of 0 miles per hour, and air temperature of 22 degrees Celsius. The hopper was also assumed to be clean and empty for each analysis. The DEM domain size was 3 meters by 0.84 meters by 3 meters, in the X (width), Y (height), and Z (length) directions.

Test Method

Field

Since grass height and cut height varied throughout testing a custom gage was primarily used to measure the height of both uncut and cut grass, Figure 30 and Figure 31, respectively. For grass heights taller than 5.5 inches, other standard measuring devices were used.



Figure 30. Grass height gage showing uncut grass to be about an average of 3.25 inches.



Figure 31. Grass height gage showing cut grass to be about an average of 2.25 inches.

The cut plots were 100 feet wide and due to variations in grass conditions, cut heights, and ground speeds on any given test day, the number of runs made would vary.

Typically, one run would equal one to three passes along the width of the cut plot. On occasion, one run would equal up to four total passes. Speeds and cut heights were changed between tests to give different loadings on the deck and MCS. This helped drive differentiation between test models.

Two primary methods of testing were conducted. The first method was to let the lowest performing unit set the pace during testing. The second method was to let the highest performing unit set the pace during testing. Each method has its advantages. The first method levels the playing field and keeps the other units from immediately outperforming the lowest performing unit, giving a sense of performance of the least performing unit. With the highest performing unit setting the pace, the immediate differentiation in performance could be observed.

Virtual

Neumorous locations were monitored or observed during each virtual DEM simulation. The primary monitoring location was at the discharge chute exit. A monitoring box that was 50 millimeters deep and the width and height of the discharge chute exit was placed to monitor average particle velocity. Two primary observation locations were the lower discharge chute entrance (after the nozzle) and the back of the MCS hopper. The lower discharge chute entrance was observed for material buildup while the back of the hopper of observed for material dispersion. The monitoring location can be viewed in Figure 32 and the three observation locations can be viewed in Figure 33.

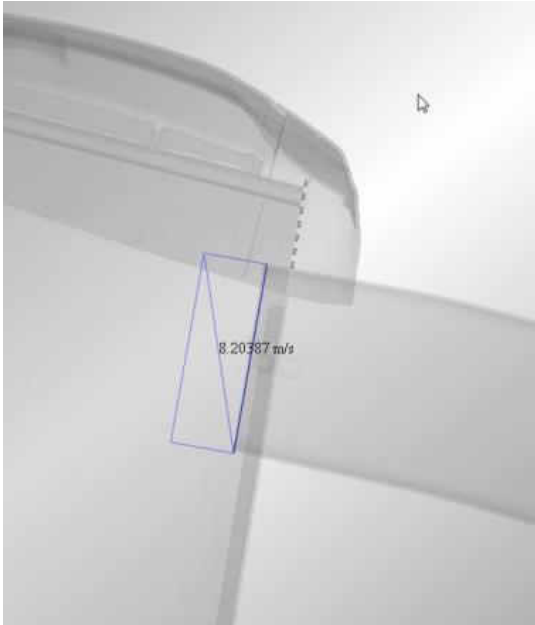


Figure 32. Particle velocity monitoring location. Located at MCS chute exit inside the hopper.

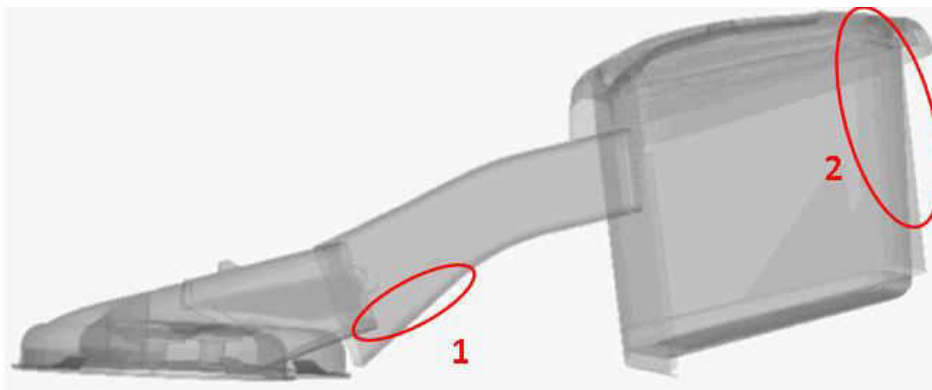


Figure 33. Observation locations for material buildup and dispersion. 1) Lower discharge chute entrance. 2) Back face of hopper.

Results – Field & Virtual

As previously mentioned in the test method section, cut heights and grass heights were varied during field testing. This was done to produce various loadings on the models which in turn produced model differentiation. This was needed in order to make test runs in the short window where conditions were still considered to be “steady-state”.

For the sake of computation time and energy spent on virtual analysis, one grass type and one primary grass length of 35 millimeters was used during all the DEM simulations.

Baseline 1

As previously mentioned about the B1 model, there is a gap created as cut height increases between the lower portions of the deck chute and MCS chute causing a wake region. It was shown in the DEM simulation of this model that particles would fall out of suspension as they neared this wake region. The low velocity particles would then stick to the lower entrance of the discharge chute and begin building up. This same observation was made in the field. Over a small period of time, particles would fill the gap between the two chutes and continue building in the entrance of the discharge chute. The buildup of particles would move forward into the lower chute and ultimately, complete plugging of the lower chute would occur. The initial buildup of particles from the DEM model can be viewed in Figure 34 below.



Figure 34. Beginning stages of material buildup in the B1 model discharge chute.

Two distinct particle flow streams were also observed in the DEM model. One followed the top of the lower chute and the other followed the bottom of the lower chute.

These two flow streams and the material dispersion at the back of the hopper can be viewed in Figure 35.

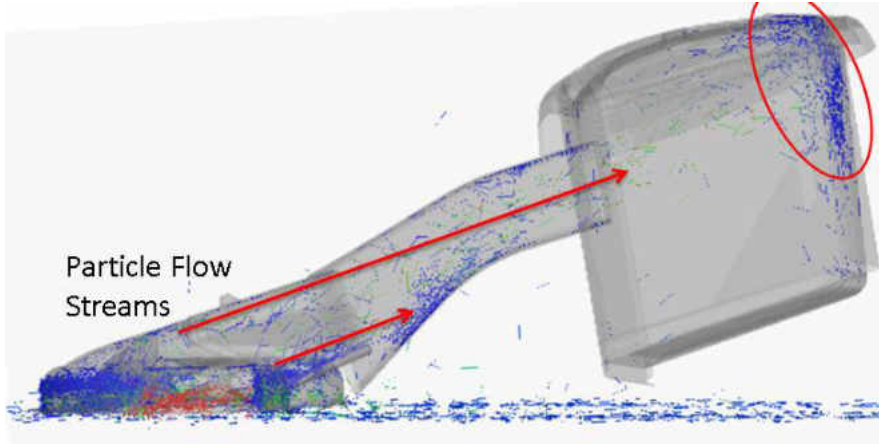


Figure 35. B1 model DEM snapshot showing particle streams into the discharge chute and the material dispersion at the back of the hopper.

At this time it was thought the buildup of material at the discharge chute entrance was directly caused by the wake region between the upper and lower chutes.

Baseline 2

It wasn't until B2 that the attack angle of the lower chute showed to be of great importance. With the wake region removed from B1 and more controlled air velocities of the B2 design, it was thought that the discharge chute would direct the particles into the hopper. It was shown in the DEM simulation of the B2 model that particles would quickly build up in the lower portion of the MCS chute. The particles exiting the lower half of the deck chute were being directed immediately into the bottom curvature of the MCS chute and would stick, not deflect. This was also observed during field tests with large or wet particles. Figure 36 shows the initial buildup of particles from the DEM model.

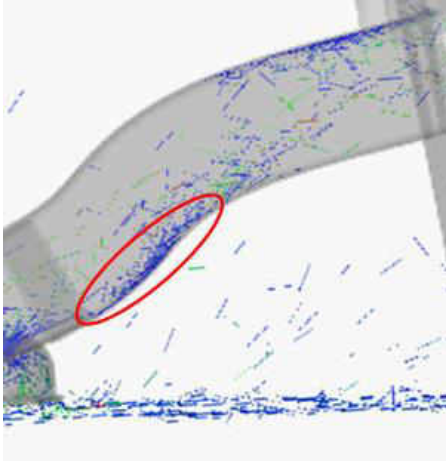


Figure 36. Beginning stages of material buildup in the B2 model discharge chute.

Two distinct particle flow streams were also observed in the DEM model. One followed the top of the lower chute and the other followed the bottom of the lower chute. However, compared to the B1 model, these two flow streams are directed into the bottom surface of the discharge chute. These two flow streams and the material dispersion at the back of the hopper can be viewed in Figure 37.

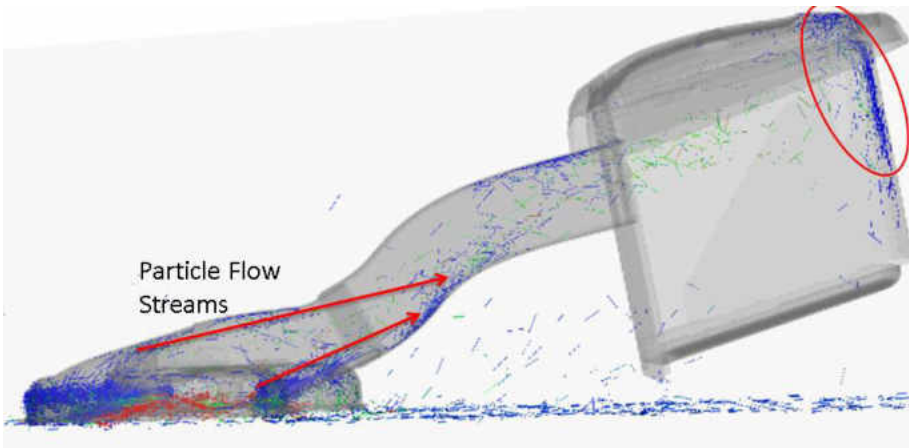


Figure 37. B2 model DEM snapshot showing particle streams into the discharge chute and the material dispersion at the back of the hopper.

It was then realized after this model that attack angle played a very important role in particle flow. The discharge chute geometry also needed to be designed in such a way as to limit any hindrances imparted to particle flow.

Iteration 1

The Iter1 model was a large improvement to bagging performance over the B1 and B2 models. No immediate buildup in the discharge chute entrance was observed in the DEM simulation of the Iter1 model. However, the bottom surface of the lower chute had a small pocket inherent in the design. This small pocket allowed for material buildup in a short period of time. This same material buildup was observed in the field testing of Iter1. There was no buildup of dry material however; wet material would immediately fill in the pocket of the lower chute. The initial material buildup in the lower chute entrance and the pocket in the lower chute can be viewed in Figure 38 below.

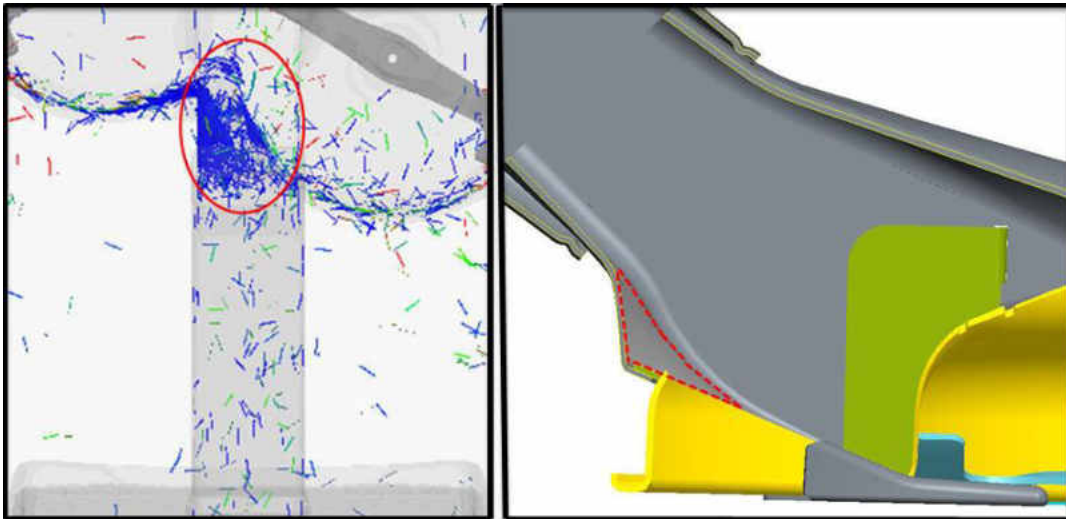


Figure 38. Beginning stages of material buildup in the Iter1 model lower chute, left. The lower chute curvature or pocket can be seen on the right.

With the increased attack angle and new discharge chute geometry of the Iter1 model, particles were not launched immediately at the bottom surface of the discharge chute. This showed to be highly effective in getting material from the mower deck to the hopper. As can be seen in Figure 39, particle flows are immediately directed part way into the upper chute. These flow paths cross approximately half way through the chute system. It was also observed with the Iter1 model that particle distribution was also shifted to a lower position at the back of the hopper.

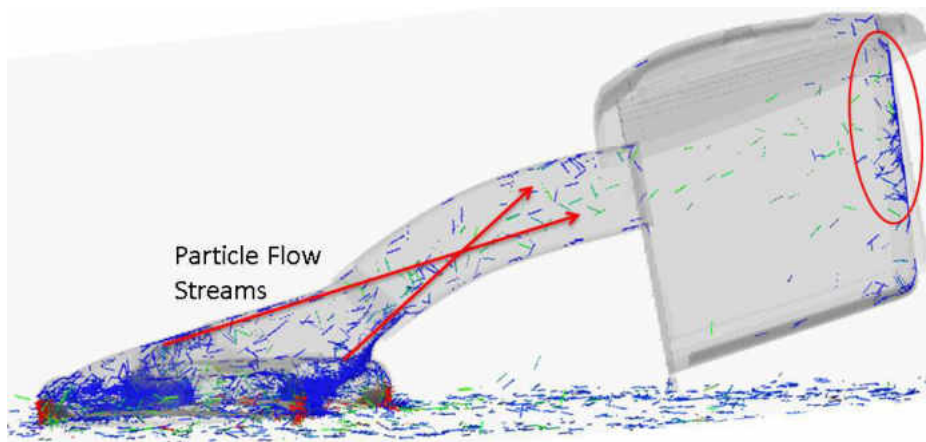


Figure 39. Iter1 model DEM snapshot showing particle streams into the discharge chute and the material dispersion at the back of the hopper.

Iteration 2

Bagging performance was further increased with the removal of the lower chute pocket. No accumulation was observed in the discharge chute entrance however, accumulation was observed on the winkle picker during the DEM simulation of the Iter2 model. This was also observed during field testing in limited conditions. During heavy, high moisture content loadings was buildup observed in this area. Lighter, wet or dry loadings, no buildup was observed. The initial material buildup at the winkle picker can be viewed in Figure 40 below.

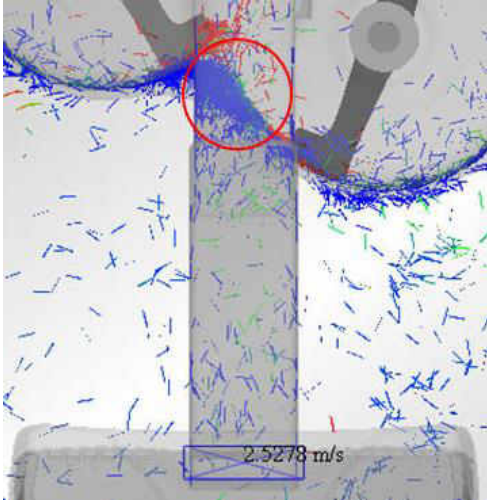


Figure 40. Beginning stages of material buildup on the Iter2 model winkle picker.

Even with a slightly reduced attack angle of the Iter2 model versus the Iter1 model – 38 degrees and 43 degrees, respectively – the particle flows were still directed partway up the discharge chute. These flow paths cross approximately half way through the chute system. The particle distribution remained in the same general location at the back of the hopper compared to the Iter1 model. The Iter2 particle flow streams and distribution of particles at the back of the hopper can be viewed in Figure 41 below.

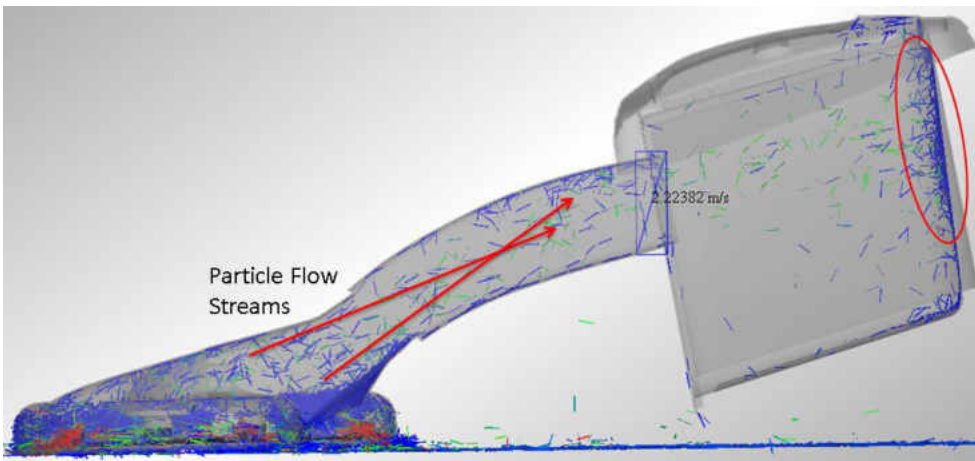


Figure 41. Iter2 DEM snapshot showing particle streams into the discharge chute and the material dispersion at the back of the hopper.

Summary

It became apparent after the B1 and B2 model simulations as well as field testing, that immediate manipulation of particles was needed in order to mitigate plugging of the lower chute and increase overall bagging performance. An increased attack angle improved particle velocities of the Iter2 model. Particle distribution was much more uniform in the Iter2 model and was attributed to the large vane between the two deck shell chambers. The increased attack angle and more uniform particle distribution greatly increased the bagging performance of the Iter2 model versus previous models.

CHAPTER VI

DISCUSSION

Grass Types, Grass Heights & Cut Heights

Although grass types vary from place to place there were three types and two mixtures that the measure of bagging performance was tested in; Rye, Blue, Fescue, a Rye/Blue mixture, and a Blue/Fescue mixture. Through various testing and experiences, Rye grass was considered to be the hardest of the grass types tested to bag, especially when it has been newly planted. It tends to be “stickier” than the other grass types. The number of tests conducted in each grass type can be viewed in Figure 42 below.

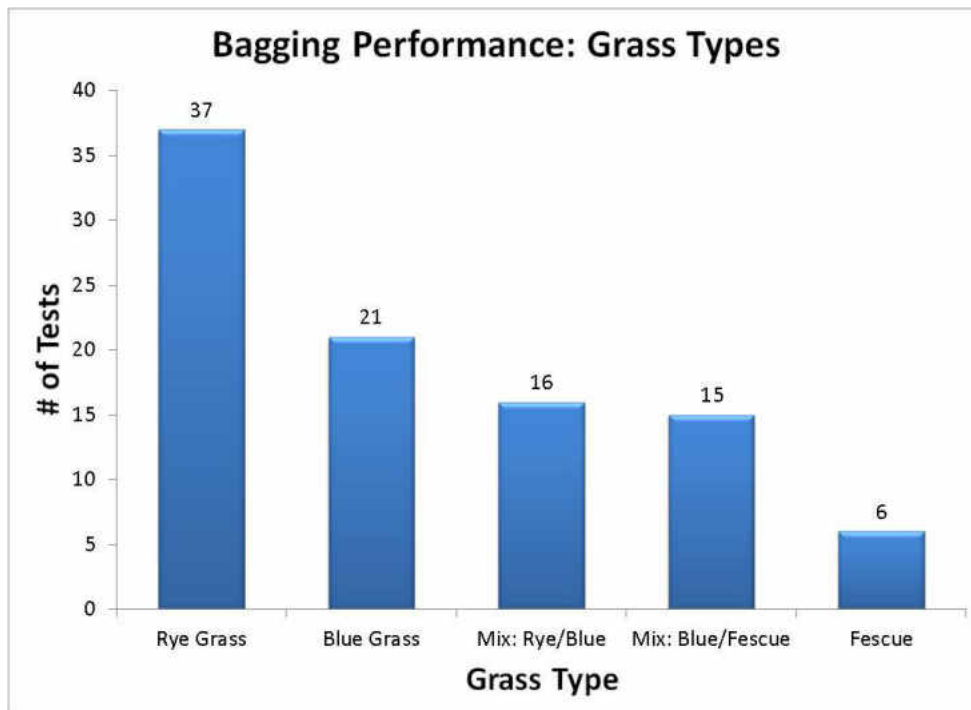


Figure 42. Number of tests run in each grass type.

A large range of grass heights was tested, ranging from as short as 1.5 inches to as tall as 14 inches. Grass heights lower than 1.5 inches were found to be difficult to maintain. The average grass heights tested in can be viewed below in Figure 43.

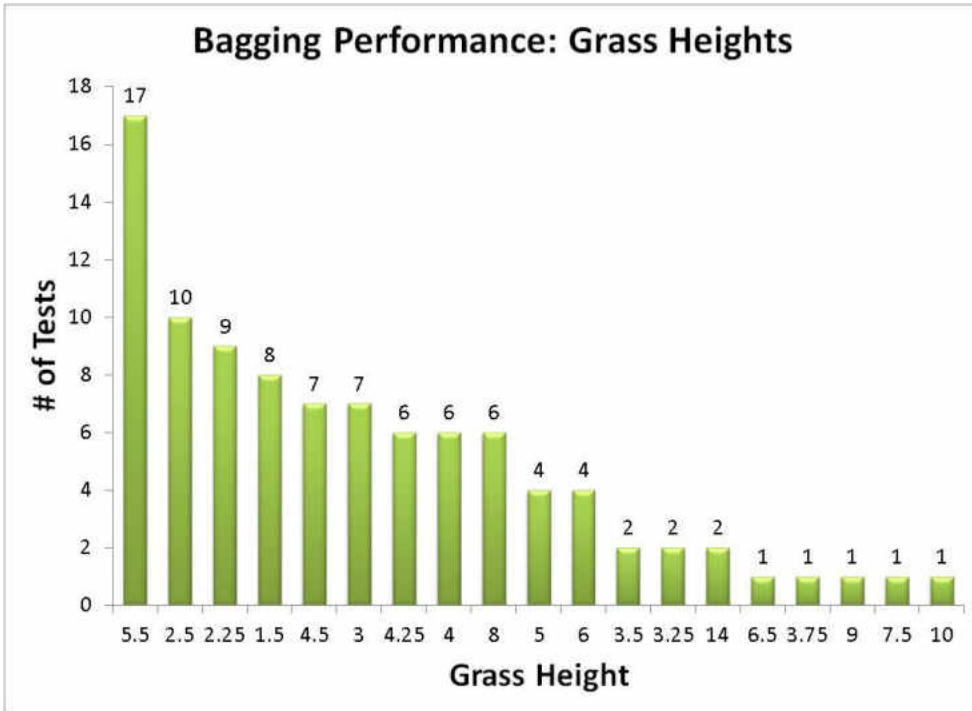


Figure 43. Number of tests run in each grass height.

At low cut heights air begins to be choked off from the deck, making it harder to bag grass. Ground speed and grass height also affect air entering the deck due to the increased amount of grass needing to be processed. To combat this, the deck rake was increased between the B1 and Iter1 models, from 6 to 10 millimeters, respectively. A look at the various heights of cut used during testing can be seen in Figure 44 below.

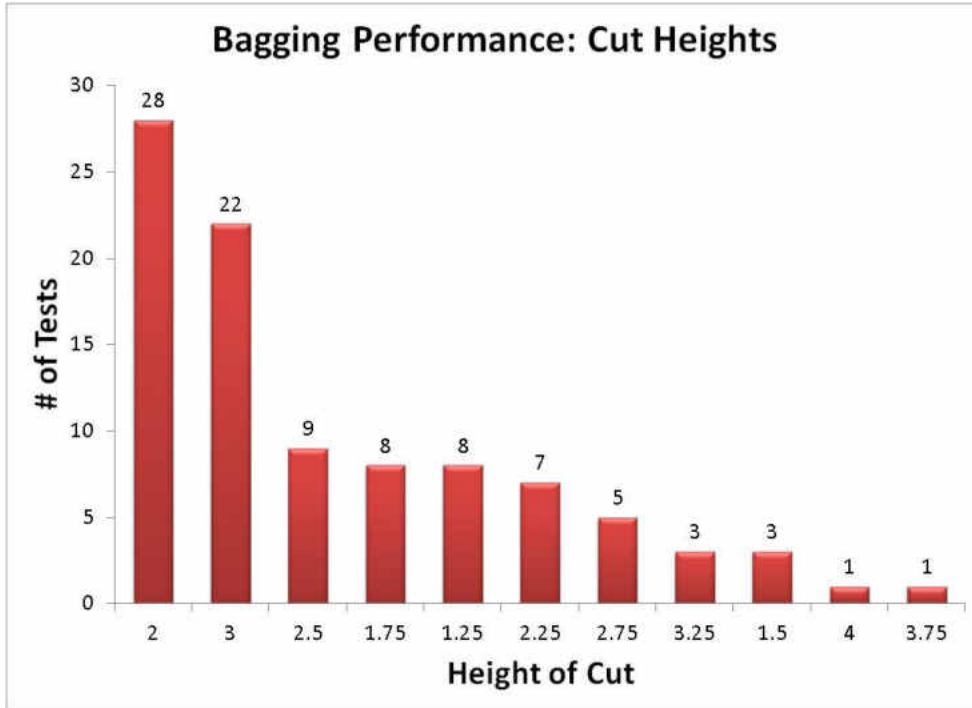


Figure 44. Number of tests run at each height of cut.

A total of 95 individual tests were conducted across the four models. The tests were run in pairs, as mentioned before with two field test methods; two models running side-by-side being recorded as two tests.

MCS Chute Exit Particle Velocities

Previously shown in Figure 32, the average particle velocity was monitored at the exit of the MCS chute during the DEM simulations. Data points were collected every 0.1 seconds up to 1 second for each model with the 35 millimeter grass length. It took 0.2 seconds for grass particles to enter the monitoring box. Therefore, no data was recorded for the 0.1 and 0.2 data points. The individual data points as well as the graph can be viewed in Table 6 and Figure 45 below.

Table 6. Average particle velocity at the MCS chute exit for each model.

Average Particle Velocity at MCS Chute Exit (m/s)				
Time (sec)	Baseline1 35mm	Baseline2 35mm	Iter1 35mm	Iter2 35mm
0.3	12.73	9.29	7.64	10.99
0.4	12.31	8.87	6.67	8.84
0.5	11.90	4.27	7.59	9.60
0.6	6.65	6.89	7.9	8.76
0.7	11.04	5.33	7.63	7.14
0.8	8.22	7.90	7.79	5.01
0.9	8.83	8.05	9.42	5.91
1	7.84	7.52	8.20	6.97
Average	9.94	7.27	7.85	7.90

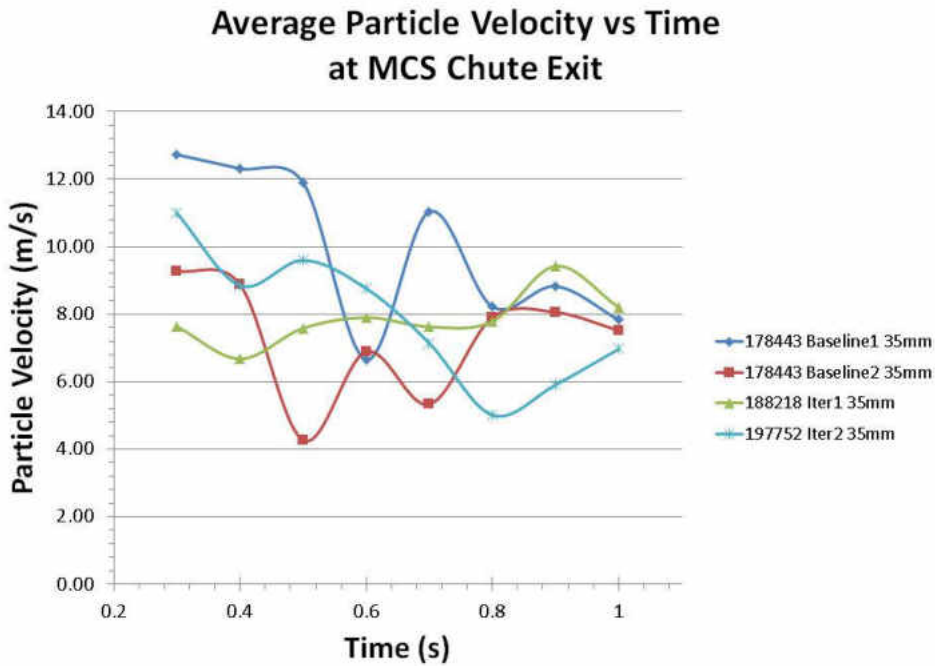


Figure 45. Graphical view of DEM data points of average particle velocity at the MCS chute exit for each model.

Room for Improvement & Future Opportunities

Several opportunities or room for improvement were identified throughout this project to further advance bagging performance research. They are listed below.

- Collect data on multiple grass conditions for input into DEM simulations.
 - This could help improve correlation between DEM simulations and field test observations.
- Collect data on various particle sizes for input into DEM simulations.
- Test multiple particle sizes simultaneously within DEM simulations.
 - This could give a more “real world” simulation.
- Further develop the process and method for collecting air flow data in the field.
 - This could lead to more accurate field data
- Further post processing of existing DEM models.

CHAPTER VII

CONCLUSION

In summary, field research has been conducted to gain a better understanding of any and all factors involved as well as what factors can be controlled, what factors are uncontrollable, and what factors can be held constant or at least mitigated. Computational Fluid Dynamics (CFD) and Discrete Element Method (DEM) simulations have been used to aid in geometry factor identification, field data validation, and field performance predictions.

During this study, a path was identified that leveraged the airflow generated by the mower blades through the MCS and mower deck chutes, in moving cut grass from the mower deck to the hopper. This path showed that immediate manipulation of both the air and grass particles needed to occur in order to increase bagging performance; this was done at the lower chute and by the lower chute attack angle. This path also showed that the MCS chute should only act as a guide, not forcibly directing air and particle flow.

Further development of the airflow in both the MCS and deck chutes has aided in increased bagging performance and decreased plugging during those heavy, wet mowing conditions. Consequently, a better understanding of the CFD and DEM models has resulted in improvements to future model analyses and better field performance predictions.

APPENDICES

Appendix A
Model Information

In Table 6 below, much of the common information between models used throughout the report can be viewed.

Table 7. Model information.

Model Information					
Model	Units	B1	B2	Iter1	Iter2
Blade Type	--	J-Wing	J-Wing	J-Wing	J-Wing
Blade Tip Speed (Nom.)	FT/MIN	15,717	15,717	15,717	15,717
V-Baffle	Y/N	Y	Y	Y	Y
Vane	Y/N	N	N	Y	Y
Deck Rake	MM	6	6	10	10
Deck Chute Attack Angle	DEG	22	28	43	38
Deck Chute Exit Area	MM ²	3.47E+04	3.16E+04	2.97E+04	3.05E+04
MCS Chute Exit Area	MM ²	3.67E+04	3.97E+04	3.87E+04	3.83E+04
Chute Exit Area Ratio	--	1.06	1.26	1.31	1.26
Back Plate Venting Area	MM ²	3.96E+04	3.96E+04	2.16E+04	2.16E+04
Hopper Size	Liter	270	270	270	270
Avg CFD Air Nozzle Exit Velocity	M/S	20.5	20.3	20.8	23.4
Avg Test Air Nozzle Exit Velocity	M/S	18.0	25.5	23.4	23.4
Avg CFD Air MCS Exit Velocity	M/S	18.6	17.7	15.5	18.2
Avg Test Air MCS Exit Velocity	M/s	17.3	19.9	18.6	18.3

Appendix B CFD Cross-Section Results

As can be seen with the side-by-side comparison of the nozzle and MCS chute cross sections in Figure 46, an increase in overall velocities was observed. With the addition of the vane in Iter1 and a larger vane in Iter2, the counter-clock-wise spiral of air and particles between the nozzle and MCS chute sections in B1 and B2 was eliminated.

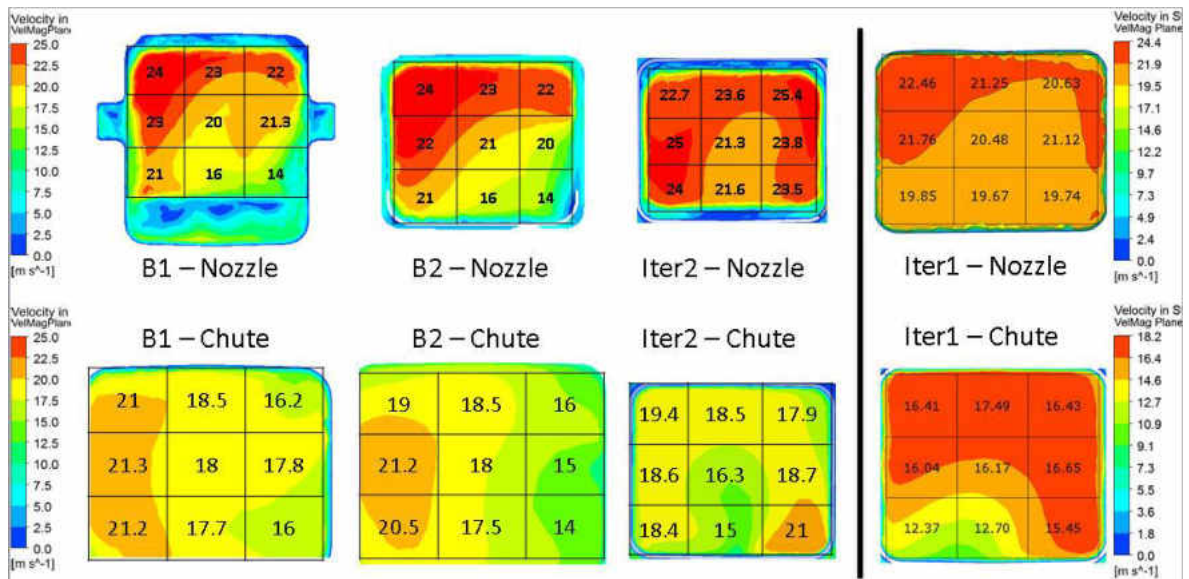


Figure 46. CFD cross-section results compared side by side.

Appendix C
Grass Type, Grass Height & Cut Height Percentage Breakdown

A percentage breakdown of testing conducted in each of the grass types, various grass heights, and various cut heights can be viewed in Table 8, Table 9, and Table 10, respectively.

Table 8. Percentage breakdown of number of tests conducted in each grass type.

	Grass Type	# of Tests	% of Total
	Rye Grass	37	38.9%
	Blue Grass	21	22.1%
	Mix: Rye/Blue	16	16.8%
	Mix: Blue/Fescue	15	15.8%
	Fescue	6	6.3%
Total	5	95	100%

Table 9. Percentage breakdown of number of tests conducted at each height of cut.

	Height of Cut	# of Tests	% of Total
	2	28	29.5%
	3	22	23.2%
	2.5	9	9.5%
	1.75	8	8.4%
	1.25	8	8.4%
	2.25	7	7.4%
	2.75	5	5.3%
	3.25	3	3.2%
	1.5	3	3.2%
	4	1	1.1%
	3.75	1	1.1%
Total	11	95	100%

Table 10. Percentage breakdown of number of tests conducted in each grass height.

Grass Height	# of Tests	% of Total
5.5	17	17.9%
2.5	10	10.5%
2.25	9	9.5%
1.5	8	8.4%
4.5	7	7.4%
3	7	7.4%
4.25	6	6.3%
4	6	6.3%
8	6	6.3%
5	4	4.2%
6	4	4.2%
3.5	2	2.1%
3.25	2	2.1%
14	2	2.1%
6.5	1	1.1%
3.75	1	1.1%
9	1	1.1%
7.5	1	1.1%
10	1	1.1%
Total	19	95
		100%

Appendix D Other CFD Data

Several other pieces of data observed and collected during CFD was the lift component of velocity just above the mower blade wing and pressure sampled through a sizeable control volume within the main area of the hopper. These can be seen in Figure 47 and Figure 48, respectively. There is currently no method for measuring air or particle flow data within the deck shell due to safety concerns.

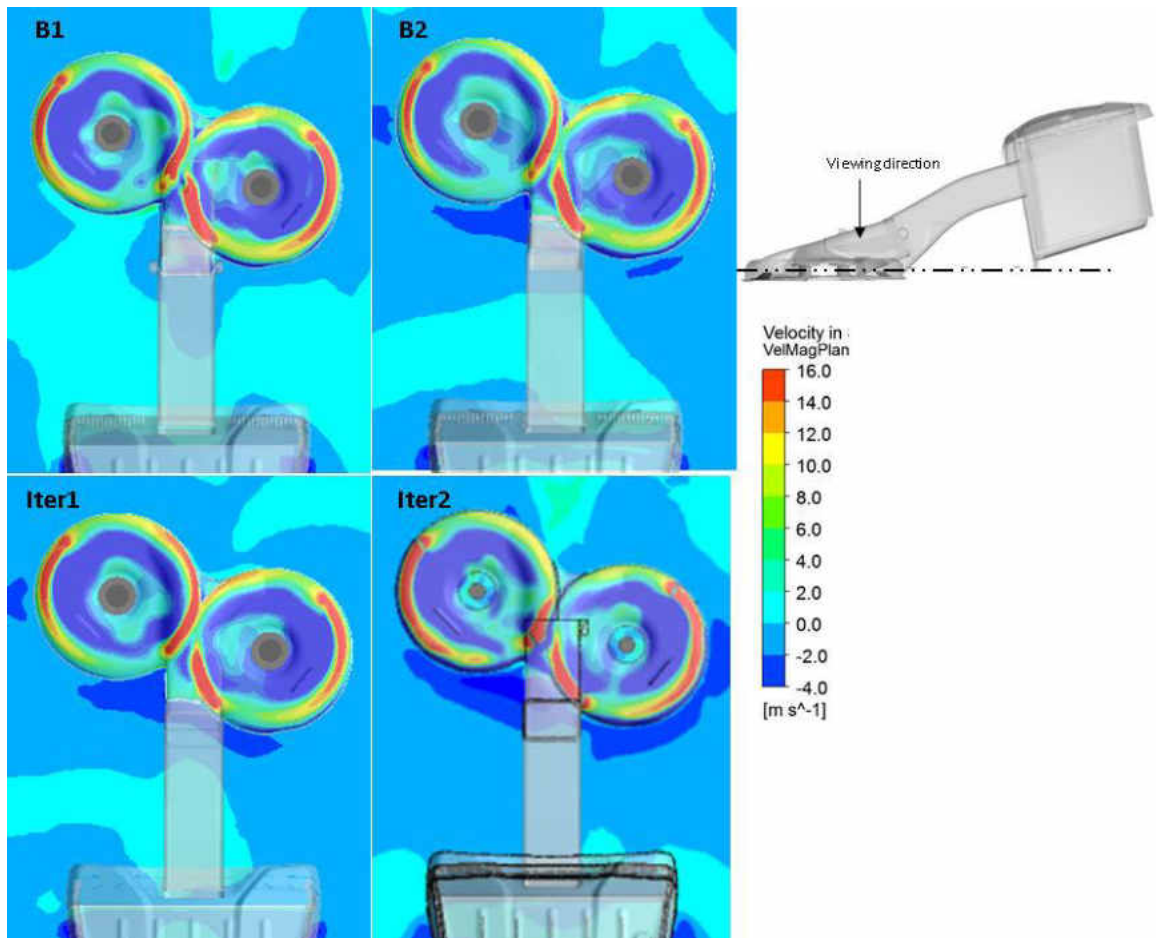
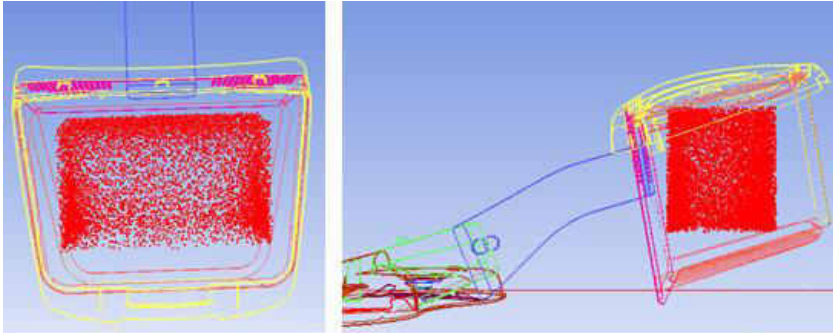


Figure 47. Lift component of velocity above the HoC.



S No	Case	Average Static Pressure (Pa)
1	B1	52.83
2	B2	38.46
3	Iter1	85.01
4	Iter2	85.00

Figure 48. Average pressure sampled in the hopper.

Appendix E CFD Process Summary

In describing the four CFD test models for Understanding and Predicting Bagging Performance Through the use of CFD and DEM Simulations, each model was setup in the same manner. Each model started life as a full 3D parametric model representative of what is manufactured. The models were “slimmed down” by removing componentry and features that have no effect on the CFD. For example, almost all assembled or welded components are removed. Also, holes, slots, splines and other unnecessary protrusions are removed. The main reasons for this are to: reduce meshing in the CFD model and to reduce CFD setup times. By reducing mesh, you reduce equations and therefore solve times. Without “de-featuring” of the parametric model, one would have to define every hole and slot that air could pass through on a solid model, thus greatly increasing setup times. The CFD team takes this a step further by filling in all gaps between components due to manufacturing and part tolerances. As an example, look at Figure 49 below to see how the parametric model of the mower deck shell is “de-featured”.

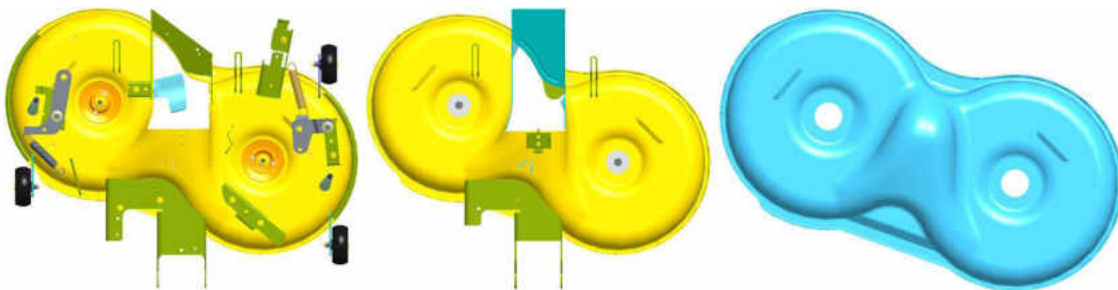


Figure 49. Parametric “de-featuring” of the mower deck shell.

The second step is to setup the bounding box and mower blade control volumes. The bounding box is the air control volume for the entire model. This is done in the 3D parametric space prior to importing into the CFD software. In all four test models, the

bounding box was held constant. It was 3 meters by 2 meters by 3 meters in the X (width), Y (height), and Z (length) directions. Meshing of the air also needs to take place, so you don't want the bounding box too big however, you don't want it too small either. If the box is oversized, your mesh count is high and the computation time increases. If the box is too small, you risk high velocity air circulation, (high velocity air from one section which would otherwise be slow moving or stagnant, gets ingested into another section) which could affect the CFD results. The mower blade control volumes are created to be the exact diameter and height of the blade. This gives the interface between the physical blade and the bounding box. The below figure will give you an idea of the bounding box size compared to the model size. It also shows the mower blade control volumes.



Figure 50. CFD bounding box and mower blade control volumes.

Step three is to import the final parametric model, with the bounding box and blade control volumes, into the CFD software and setup the specific CFD parameters. All CFD inputs were held constant from model to model, as the goal was to test the theories and geometry relating to bagging performance, not specific inputs. Since the hopper bag itself was kept constant between models, the same airflow versus pressure drop data was used for the hopper bag screens. This data is imported and applied to the individual bag screens within the CFD program. One assumption that is made with respect to the hopper

is that it is clean and empty. Below is a list of several other inputs applied to each CFD model. These inputs were based on how field test data was collected.

- Mower Blade Speed: 2,850 revolutions per minute
- Height of Cut: 3.25 inches
- Wind Speed: 0 miles per hour
- Air Temperature: 22 degrees Celsius
- Ground Speed: 0 miles per hour

Once all inputs are defined, the model is meshed. After meshing is completed the model is solved. Once the CFD model is solved, it is post-processed. This is where the CFD team gathers all the information requested. The CFD team also points out trends or patterns as well as other observations such as significant velocity and pressure changes, wake and recirculation regions, etc. A list of what is requested has been detailed below.

- 24 cross-section views throughout the model showing velocity magnitude
- 3 cross-section views showing the lift component of air around the mower deck
- 4 cross-section views showing pressures
- 2 cross-section views showing velocity magnitude at the field data collection locations
- Sampled hopper pressure

REFERENCES

- [1] W. Chon and R.S. Amano, "Investigation of Flow Behavior around Corotating Blades in a Double-Spindle Lawn Mower Deck," *International Journal of Rotating machiner*, vol. 2005, no. 1, pp. 77-89, 2005.
doi:10.1155/IJRM.2005.77

- [2] JimQ. "husqvarna combi deck...any good?" Online posting. 21 Aug. 2008.
Commercial & Residential Lawn Mowing.
Web Forum. 5 May. 2015 <<http://www.lawnsite.com/showthread.php?t=243264>>

- [3] PTC, Inc. (2014). *PTC Creo Parametric*. Retrieved from PTC: <http://www.ptc.com>

- [4] CD-adapco. (2014). *Star-CCM+*. Retrieved from CD-adapco: <http://www.cd-adapco.com>

- [5] DEM Solutions. (2014). *EDEM Software Platform*. Retrieved from DEM Solutions:
<http://www.dem-solutions.com>

- [6] Dwyer Instruments, Inc. (2014). *Air Velocity Measurement*. Retrieved February 2014,
from Dwyer Instruments, Inc.: <http://www.dwyer-inst.com>